Systems-based approach for optimization of a scalable bacterial ST mapping assembly-free algorithm

Natasha Pavlovikj[1¶], Joao Carlos Gomes-Neto[2,3¶], Jitender S. Deogun[1], Andrew K. Benson[2,3*]

[1] Department of Computer Science and Engineering, University of Nebraska-Lincoln, Lincoln, Nebraska, United States of America

[2] Department of Food Science and Technology, University of Nebraska-Lincoln, Lincoln, Nebraska, United States of America

[3] Nebraska Food for Health Center, University of Nebraska-Lincoln, Lincoln, Nebraska, United States of America

* Corresponding Author:

E-mail: abenson1@unl.edu (AKB)

¶ These authors contributed equally to this work.

Abstract

Epidemiological surveillance of bacterial pathogens requires real-time data analysis with a fast turn-around, while aiming at generating two main outcomes: 1) Species level identification; and 2) Variant mapping at different levels of genotypic resolution for population-based tracking, in addition to predicting traits such as antimicrobial resistance (AMR). With the recent advances and continual dissemination of whole-genome sequencing technologies, large-scale population-based genotyping of bacterial pathogens has become possible. Since bacterial populations often present a high degree of clonality in the genomic backbone (i.e., low genetic diversity), the choice of genotyping scheme can even facilitate the understanding of ancestral relationships and can be used for prediction of co-inherited traits such as AMR. Multi-locus sequence typing (MLST) fits that purpose and can identify sequence types (ST) based on seven ubiquitous genome-scattered loci that aid in genotyping isolates beneath the species level. ST-based mapping also standardizes genotyping across laboratories and can be consistently used worldwide. However, ST-based algorithms, when using Illumina paired-end sequences, often rely on genome assembly prior to classification. That hinders rapid genotyping and scalability which are essential aspects of genomic epidemiology. stringMLST is a kmer-based ST method with the capacity to solve both hurdles. Yet, a comprehensive scalable comparison of its use in contrast to a standard MLST program for a wide array of phylogenetically divergent Public Health-relevant bacterial pathogens is lacking. Herein, we first demonstrated that stringMLST is a fast tool that can be deployed for ST-based epidemiological

47 inquiries of bacterial populations. Additionally, we systematically evaluated and
48 showed the impact of genome-intrinsic and -extrinsic features, as well as the
49 optimal kmer length in maximizing the performance of stringMLST on species-
50 by-species basis, and highlighted a few instances where this program may not be
51 applicable in its current format. Furthermore, we integrated stringMLST as part of
52 our freely available and scalable hierarchical-based population genomics platform
53 called ProkEvo. Besides facilitating automatable and reproducible bacterial
54 population guided analysis, ProkEvo now offers a rapidly deployable genomic
55 epidemiology tool for ST mapping, with specific guidance on how to optimize its
56 performance, that can be widely applicable by microbiological laboratories and
57 epidemiological agencies.
58

59 Introduction

60 Modern epidemiological investigation of bacterial pathogens is primarily focused
61 on real-time, fast turn-around characterization of many thousands of isolates,
62 routinely received by Public Health laboratories and regulatory agencies [1][2].
63 Additionally, due to the large-scale availability of whole-genome sequencing
64 (WGS) and an emerging emphasis on retrieving accurate metadata, three major
65 goals can be achieved with population-based inquiries: 1) Species identification;
66 2) Genotyping at different levels of hierarchical resolution; and 3) Prediction of
67 co-inherited traits such as antimicrobial resistance (AMR) via loci mapping, or
68 based on the assessment of population-inherited linkage between the core- and
69 accessory-genomes [3]. In general, bacterial populations contain a genomic

70 backbone (i.e., clonal-frame), for which the degree of clonality is predicted to be a
71 heritable trait, leading to a measurable degree and pattern of co-inheritance
72 between core- and accessory-genes (loci) – high *linkage disequilibrium* (LD)
73 [4][5][6][7]. Core loci are those found in 99% of the genomes or more; whereas
74 accessory loci represent a sparse ensemble present in less than 99% of genomes,
75 which combined form the species-specific pan-genomic content [66]. In theory,
76 one should be able to identify a genotyping scheme that not only facilitates
77 sufficient isolate differentiation beneath the species level, but can also reveal the
78 pattern of population diversification and structuring, while being used in
79 phenotypic prediction such as for AMR traits. This optimal level of genotypic
80 resolution can be considered an informative genotypic unit that facilitates both
81 ecological and epidemiological inquiries.
82 Multi-locus sequence typing (MLST) is a well-established and widely used
83 genotyping technique that classifies bacterial genomes into sequence types (ST)
84 [8]. ST classification is achieved by mapping seven ubiquitous genome-scattered
85 loci using highly curated, and species-specific allelic databases. Essentially,
86 sequences for those seven loci can be generated by polymerase chain reaction
87 (PCR)-based assays, or WGS [8][9][44]. Regardless of the methodology, partial
88 sequences for each locus are mapped against multiple ever-expanding public
89 allelic databases [27][30][67]. The combination of all seven allelic numbers
90 defines which ST number the isolate is classified into. ST-based classification
91 provides useful genotyping approach below the species level, while revealing the
92 population structure and retrieving ancestral relationships, since when five or

93 more loci are identical to one another between two genomes, both belong to the
94 same clonal complex (i.e., group of STs that have shared a common ancestor very
95 recently) [8][9][28][44]. Moreover, ST-based genotyping standardizes the
96 nomenclature for intra- and inter-laboratorial diagnostics and epidemiological
97 inquiries worldwide [9][10][11]. Lastly, genes that are part of the MLST scheme
98 can co-vary with other accessory loci important for phenotypic predictions such
99 serotyping (e.g., *Salmonella enterica*) and inter-species AMR predictions
100 [12][13][14].

101 Harnessing this intrinsic LD property of bacterial pan-genomes has been the
102 basis for recent innovation in epidemiological investigations, whereby heuristic
103 mapping of STs led to accurate prediction of AMR profiles [14][15]. However,
104 ST-based classification, using the most widely distributed Illumina sequencing
105 technology, is often dependent on genome assemblies [27][30][67]. That results in
106 slower turn-around for data analysis and hinders ST-based surveillance efforts for
107 enhancing scalability when working with many thousands of genomes [16][21].
108 One approach to overcome those hurdles is to use kmer-based ST classification
109 directly from Illumina paired-end raw reads (assembly-free). stringMLST is an
110 approach that successfully accomplishes that goal [17], but has not yet been
111 systematically tested for its analytical performance while classifying thousands of
112 genomes from phylogenetically divergent bacterial pathogens.

113 Therefore, the purpose of this work was to test whether stringMLST can be
114 used as a rapid and accurate replacement of the standard MLST programs for
115 scalable genotyping of phylogenetic divergent bacterial pathogens, with direct

Public Health implications, using Illumina raw sequences. In contrast to the original work [17], our systematic approach demonstrated a comprehensive comparison between a standard MLST program vs. stringMLST, while classifying many thousands of genomes across 15 pathogens, including: *Acinetobacter baumannii (*Phylum: Proteobacteria)*, Clostridioides difficile (*Phylum: Firmicutes)*, Enterococcus faecium (*Phylum: Firmicutes)*, Escherichia coli (*Phylum: Proteobacteria)*, Haemophilus influenzae (*Phylum: Proteobacteria)*, Helicobacter pylori (*Phylum: Proteobacteria)*, Klebsiella pneumoniae (*Phylum: Proteobacteria)*, Mycobacterium tuberculosis (*Phylum: Actinobacteria)*, Neisseria gonorrhoeae (*Phylum: Proteobacteria)*, Pseudomonas aeruginosa (*Phylum: Proteobacteria)*, Streptococcus pneumoniae (*Phylum: Firmicutes)*, Campylobacter jejuni* (Phylum: Proteobacteria), *Listeria monocytogenes (*Phylum: Firmicutes), *Salmonella enterica* (Phylum: Proteobacteria), and *Staphylococcus aureus* (Phylum: Firmicutes). Additionally, we have also analyzed the optimal kmer length for 23 most relevant zoonotic serovars of *Salmonella enterica* subsp. *enterica* lineage I (*S. enterica*) individually given its cryptic population structure and diverse ecology [12]. For comparison between programs, we use the following analytical outcomes as proxies for algorithmic performance-based assessment: 1) Computational runtime and memory used for genome classification; 2) ST richness and diversity metrics; and 3) Proportion of non-classified STs and concordance between programs. [17]Importantly, we measured the statistical contribution of genome-intrinsic (genome size and composition) and -extrinsic (ST database size) factors on classification accuracy at species level of

resolution, including the identification of the optimal kmer length per species. This comprehensive approach revealed how stringMLST is a deployable ready-to-use program that can be further optimized (parameter fine-tunning) based on the species dataset, while attempting to scale its application for practical implementation in microbiological laboratories and epidemiological agencies. Lastly, we added stringMLST to our computational platform called ProkEvo, aiming at facilitating its automated, reproducible, and scalable use, in combination with other standard assembly-based hierarchical genotypic and pan-genomic mapping approaches for bacterial population genomic analyses.

Materials and methods

This systems-based comparison between mlst and stringMLST was centered at capturing their differences in computational and statistical performances, and was accomplished through the following steps: 1) Narrow-scope comparative analysis across four phylogenetic distinct pathogens species; 2) Further examination of algorithmic performance within a single ecologically diverse bacterial species; and 3) Wide-scope comparison between phylogenetic divergent pathogenic species with Public Health relevance and with databases available on pubMLST (https://pubmlst.org/) for direct contrast between stringMLST and mlst.

159 **Datasets used for narrow-scope analysis**

160 WGS data from four major bacterial pathogens, including *Campylobacter jejuni*,
161 *Listeria monocytogenes*, *Salmonella enterica* subps. *enterica* lineage I (*S.*
162 *enterica*) and *Staphylococcus aureus,* were selected to be used in this first part of
163 the study. Our basis for that choice was due to three *a priori* defined criteria: 1)
164 Select bacterial species from two main phylogenetic divergent Phyla: Firmicutes
165 (*L. monocytogenes* and *S. aureus*) and Proteobacteria (*C. jejuni* and *S. enterica*);
166 2) Select zoonotic pathogens that continually cause human illnesses worldwide
167 [18]; and 3) Consider their epidemiological relevance according to the Centers for
168 Disease Control and Prevention (CDC) [19]. Specifically for *S. enterica*, 20 of the
169 CDC most investigated serovars were represented in the dataset, which includes:
170 *S.* Agona, *S.* Anatum, *S.* Braenderup, *S.* Derby, *S.* Dublin, *S.* Enteritidis, *S.* Hadar,
171 *S.* Heidelberg, *S.* Infantis, *S.* Javiana, *S.* Johannesburg, *S.* Kentucky, *S.* Mbandaka,
172 *S.* Montevideo, *S.* Muenchen, *S.* Newport, *S.* Schwarzengrund, *S.* Senftenberg, *S.*
173 Thompson, and *S.* Typhimurium [20]. All publicly available raw paired-end
174 Illumina reads for these organisms were downloaded from NCBI using parallel-
175 fastq-dump [58]. Genomes used for all analyses were randomly selected from a
176 previously downloaded samples of isolates containing *C. jejuni* (n = 21,919
177 genomes), *L. monocytogenes* (n = 19,633 genomes), *S. enterica* (n = 25,284
178 genomes), and *S. aureus* (n = 11,990 genomes) that were processed through the
179 computational platform ProkEvo [21]. Specifically, our study design was
180 comprised of random sampling of 600 genomes from each species, except for *S.*
181 *enterica* for which 600 genomes were randomly drawn per serovar (list of all 20

182 serovars is shown in S1 Table). For each species and all *S. enterica* serovars, all
183 ~600 genomes were randomly split into three independent batches, with ~200
184 genomes each. The batches were created to measure the degree of variation in
185 classification accuracy when comparing the two ST-based genotyping programs.
186 While for the majority of *S. enterica* serovars there were a total of 600 genomes
187 available, the total number of raw reads publicly available on NCBI and
188 ultimately used for the analyses for *S.* Agona, *S.* Derby, *S.* Johannesburg, *S.*
189 Mbandaka and *S.* Senftenberg was 565, 590, 534, 535 and 563 respectively. The
190 final total number of genomes used per species was: *C. jejuni* (n = 600), *L.*
191 *monocytogenes* (n = 600), *S. enterica* (n = 11,787), and *S. aureus* (n = 600). Text
192 file containing all genome NCBI SRA identifications is available here,
193 https://figshare.com/articles/dataset/_/16735411.
194

195 # Software tools

196 **mlst**

197 mlst is a standard approach for scanning genome assemblies against traditional
198 PubMLST typing schemes [22]. The genome assemblies can be in
199 FASTA/GenBank/EMBL formats [22]. mlst (version 2.16.2) was installed using
200 Anaconda, a package and environment manager that supports maintaining and
201 installing various open-source conda packages [26]. mlst uses genome assemblies
202 as an input. In order to generate assemblies from the raw Illumina paired-end
203 reads, multiple pre-processing steps were performed. Quality trimming and
204 adapter clipping were performed using Trimmomatic [50], while FastQC was

205 used to check and verify the quality of the trimmed reads [51]. The paired-end
206 reads were assembled *de novo* into contigs using SPAdes with the default
207 parameters [52]. The quality of the assemblies was evaluated using QUAST [53].
208 The information obtained from QUAST was used to discard assemblies with 0 or
209 more than 300 contigs, or assemblies with N50 value of less than 25,000 [21].
210 Finally, the assemblies that passed the quality control were used with mlst, where
211 they are categorized into specific variants based on the allele combinations from
212 seven ubiquitous, house-keeping genes [22]. A list of the exact versions of the
213 bioinformatics tools used for generating assemblies for mlst are shown on S2
214 Table. We used mlst with the default options (e.g., *mlst --legacy --scheme*
215 *<scheme> --csv <assembly.fasta> > <output>*) and the following schemes:
216 "senterica" (for *S. enterica*), "campylobacter" (for *C. jejuni)*, "lmonocytogenes"
217 (for *L. monocytogenes*), "saureus" (for *S. aureus*). The distribution of mlst comes
218 with set of pre-downloaded ST schemes. More details about these MLST
219 schemes, such as the number of alleles in the seven genes and the number of ST
220 classifications available are shown on S3 Table. To obtain the ST classifications
221 of all datasets, mlst was run as part of the computational platform ProkEvo [21].
222 Additionally, a separate run of the mlst program was used to conduct a pairwise
223 comparison between the computational performance (runtime and memory usage)
224 of mlst and stringMLST. The used mlst script can be found here,
225 https://github.com/npavlovikj/MLST_stringMLST_analyses/blob/main/scripts/ml
226 st.submit.

227

228 **stringMLST**

229 stringMLST is an assembly- and alignment-free rapid tool for ST-based
230 classification of Illumina paired-end raw reads based on kmers [17]. For the
231 analyses performed in this paper, we used stringMLST version 0.6.3. stringMLST
232 was installed using Anaconda [26]. The first step of using stringMLST was to
233 download the respective MLST scheme from PubMLST. In order to do this, a
234 species name and a kmer length were needed. The default kmer length used and
235 suggested by the developers of stringMLST for reads with lengths between 55 and
236 150 base pairs or nucleotides is 35 (common read length for Illumina paired-end
237 reads) [17]. We used stringMLST with the default options (e.g., *stringMLST.py --*
238 *getMLST --species=<species_name> -P <output_prefix> -k <kmer>*) and the
239 following species names, "Salmonella enterica", "Campylobacter jejuni",
240 "Listeria monocytogenes", "Staphylococcus aureus", and kmer lengths of 10, 20,
241 30, 35, 45, 55, 65, 70, 80, 90 independently
242 (https://github.com/npavlovikj/MLST_stringMLST_analyses/blob/main/scripts/str
243 ingMLST_dbs.submit). More details about the downloaded MLST schemes, such
244 as the number of alleles in the seven genes and the number of ST classifications
245 available are shown on S3 Table. After the MLST scheme was downloaded and
246 prepared, the final step was to run "stringMLT.py –predict" for the ST
247 classification. For this, we ran stringMLST with the databases *a priori* created and
248 the respective paired-end raw reads and kmer lengths of 10, 20, 30, 35, 45, 55, 65,
249 70, 80, 90 independently (e.g., *stringMLST.py --predict -d*

250 *<directory_raw_reads> -p -r -t -x -P <database_prefix> -k <kmer> -o*
251 *<output>*)
252 (https://github.com/npavlovikj/MLST_stringMLST_analyses/blob/main/scripts/str
253 ingMLST.submit). Our choice of using an increasing gradient of kmer lengths
254 was to evaluate whether the kmer length parameter could be optimized to enhance
255 ST-based classification accuracy across species. Lastly, stringMLST was also
256 integrated as part of the computational platform ProkEvo for a rapid ST-based
257 genotyping as part of a hierarchical genotypic scheme [21][57]. This
258 implementation can be found here,
259 https://github.com/npavlovikj/MLST_stringMLST_analyses/tree/main/Prokevo_st
260 ringMLST.
261
262 **ProkEvo-based MLST classifications**
263 In order to compare the ST-based classification accuracy and conduct other
264 statistical analysis (e.g., identifying major contributing factors influencing ST-
265 based classifications) between mlst version 2.16.2 (assembly-dependent) and
266 stringMLST version 0.6.3 (assembly-independent), all initial ST calls for all
267 selected genomes, across all four species, were done using mlst [22] through the
268 computational platform ProkEvo [21]. In brief, ProkEvo uses bacterial Illumina
269 raw paired-end sequences as an input, and the following steps are sequentially
270 done prior to ST-based genotyping using mlst: Trimmomatic for sequence
271 trimming [50], FastQC for quality control of the trimmed reads [51], SPAdes for
272 *de novo* genome assembly [52], and QUAST for quality assessment of the

genome assemblies [53]. More information on how to install and use ProkEvo for hierarchical bacterial population genomic analyses can be found here, https://github.com/npavlovikj/prokevo.

Genome-intrinsic and –extrinsic factors that can influence algorithmic performance

Both genome-intrinsic and –extrinsic factors were considered to determine their contribution on the accuracy of ST classifications when comparing mlst vs. stringMLST.

The genome-intrinsic variables considered in these analyses were: number of contigs per genome, total number of nucleotides per genome (genome length), GC% content per genome, and dinucleotide composition of genomes. The number of contigs per genome, as well as the genome length, were calculated using the assembled contigs from SPAdes [52]. The number of contigs was calculated for each genome using the Linux "grep" utility (e.g., *grep ">" assembly.fasta | wc -l*). The total number of nucleotides per genome was calculated using the "getlengths" function from the AMOS package [54]. For this analysis, we used AMOS v3.1. "getlengths" provides the length for each contig, and a custom Bash script was used to summarize these values per genome. The GC% content was calculated using the program FastQC [51]. FastQC is used to check and verify the quality of the raw Illumina paired-end raw reads. With each pair of raw reads from all datasets, FastQC v0.11 was used. One of the statistics checked for read

295 quality is GC% and this value was extracted with custom Bash script from the file
296 "fastqc_data.txt" once the FastQC output was generated. Since FastQC outputs
297 the GC% per read, the average of both reads was calculated as the final read
298 GC%. The dinucleotide composition of the genomes was calculated with the
299 function "compseq" from the EMBOSS package [55]. "compseq" calculates the
300 frequency of words of a specific length (e.g., length is 2 in the case of
301 dinucleotides) from given input genome sequences. For these analyses we used
302 EMBOSS v6.6 with the command "*compseq -word 2 -outfile <output>*
303 *assembly.fasta*" for all datasets and genomes *a priori* assembled with SPAdes
304 [52]. Next, customized Bash script was used to count the total number of
305 occurrences of each dinucleotide for each genome across all bacterial species.
306 Finally, all these outputs were merged per genome using custom Python script to
307 facilitate statistical analyses and data visualization. The used scripts can be found
308 here,
309 https://github.com/npavlovikj/MLST_stringMLST_analyses/tree/main/scripts.
310 The genome-extrinsic variables used in the analyses presented here were: the
311 total count of unique STs per database and the total count of unique alleles across
312 all seven loci used for ST classification across all bacterial species. These
313 genome-extrinsic variables were extracted from the PubMLST databases for both
314 stringMLST and mlst using custom Bash scripts. While the first step of
315 stringMLST is to download the newest available MLST scheme from PubMLST,
316 the distributed version of mlst comes with set of pre-downloaded ST and allelic
317 schemes. For each MLST scheme, the mlst distribution has a separate directory

318 with 8 files - seven are ".tfa" files with the fasta sequences of the alleles for each
319 locus, and one file (e.g., senterica.txt) contains the ST information (i.e., the total
320 number of STs mapped including their specific allelic composition across all
321 seven loci for that given species). To calculate the total number of unique STs, we
322 used the Linux utility "wc" with the text file with ST information (e.g., *wc -l*
323 *senterica.txt*). To calculate the total count of unique alleles across the seven loci,
324 the "grep" Linux utility was used with the seven ".tfa" files (e.g., *grep ">" *.tfa |*
325 *wc -l*). All calculations were done per bacterial species. The downloaded MLST
326 scheme with stringMLST is in a separate directory for each organism and used
327 kmer length. This directory had 12 files - seven are ".tfa" files with fasta
328 sequences for all alleles across all seven loci, and one file has the ST profiles
329 (e.g., Salmonella_enterica_profile.txt), while the remaining files contained
330 information about the extracted kmers and additional config and log information.
331 Similarly, the total number of unique STs for stringMLST was counted using the
332 Linux utility "wc" with the text file with ST profile information (e.g., *wc -l*
333 *Salmonella_enterica_profile.txt*) and the total count of unique alleles per loci was
334 extracted using the "grep" Linux utility with the seven ".tfa" files (e.g., *grep ">"*
335 **.tfa | wc -l*). Similarly, all ST and allelic counts were carried out per bacterial
336 species. With stringMLST, the MLST schemes are downloaded and prepared
337 separately for each different kmer length used. However, the kmer length did not
338 affect the number of STs and unique alleles per organism. Thus, these values are
339 the same across organisms and kmer lengths for stringMLST.
340

341 ## Kmer-based distribution across ST programs

342 In order to assess the potential impact of random mapping or occurrence of kmers
343 of different lengths across different bacterial species we randomly chose 100 raw
344 Illumina paired-end reads from the initial *C. jejuni*, *L. monocytogenes*, *S. aureus*
345 and *S.* Typhimurium (major representative zoonotic serovar of *S. enterica*)
346 isolates. For each read, we extracted all unique kmers of length 10, 20, 30, 35, 45,
347 55, 65, 70, 80 and 90 respectively, and counted their occurrence in the
348 corresponding raw reads. This was done using DSK v2.2.0 [56]
349 (https://github.com/npavlovikj/MLST_stringMLST_analyses/blob/main/scripts/ds
350 k.submit). Next, the total number of kmer frequency was summarized per
351 organism and kmer length, and the mean value was calculated to examine the
352 distribution of different kmers across the raw reads. For each database created
353 with stringMLST, a file with the kmer frequency for the used ST scheme was
354 generated. Using the kmers generated from the raw reads and the stringMLST
355 database, a relative frequency of the common kmers was calculated (calculated as
356 a ratio between the common kmers and the unique kmers from all the kmers
357 generated between the raw reads and the stringMLST database, e.g.,
358 *(common_kmers/unique_total_observations)*100*). The code used for this can be
359 found in our GitHub repository
360 (https://github.com/npavlovikj/MLST_stringMLST_analyses/tree/main/figures_c
361 ode).
362

Agreement in ST classification between programs

In order to assess the overall accuracy of stringMLST compared to the standard mlst approach for ST calls, a percentage of agreement in ST classification was calculated. For this, the initial dataset composed of 600 genomes from either *C. jejuni*, or *L. monocytogenes*, or *S. aureus* was selected, in addition to a total of 11,787 genomes across twenty zoonotic serovars of *S. enterica* (~600 genomes per serovar, S1 Table). The program stringMLST was run with increasing kmer lengths ranging from 10 to 90 nucleotides. If both stringMLST and mlst produced identical ST calls, either "good" or "bad" ones, the call was a match. A "good" and "bad" call represent ST with a number or a missing/blank value, respectively. The remaining combinations were classified as a mismatch. Next, the percentage of agreement (concordance) was calculated with custom R base script (https://github.com/npavlovikj/MLST_stringMLST_analyses/tree/main/figures_code).

Computational platforms

All computational analyses performed for this paper were done on Crane - one of the high-performance computing clusters at the University of Nebraska-Lincoln Holland Computing Center [23]. Crane is Linux cluster, having 548 Intel Xeon nodes with RAM ranging from 64 GB to 1.5 TB. The scalability of ProkEvo with stringMLST was tested on the Open Science Grid (OSG), a distributed, high-throughput computational platform for large-scale scientific research [24][25]. OSG is a national consortium of more than 100 academic institutions and

laboratories that provide storage and tens of thousands of resources to OSG users. These sites share their idle resources via OSG for opportunistic usage. The OSG resources are Linux-based, and due to the different sites involved, the hardware specifications of the resources are different and vary.

Computational performance

To evaluate the computational performance of stringMLST in comparison to the mlst program, we assessed the runtime and memory usage of both programs. For this, we chose four different datasets, *C. jejuni*, *L. monocytogenes*, *S. aureus* and *S.* Typhimurium (major representative zoonotic serovar of *S. enterica*), with three different batches of 200 genomes each, with a total of 600 genomes each. We ran mlst with all required steps, such as quality trimming and adapter clipping, *de novo* assembly and assembly discarding on each dataset (see Section Software tools: mlst for more detailed description). Separately, we ran stringMLST with a range of 10 different kmer lengths (10, 20, 30, 35, 45, 55, 65, 70, 80, 90) on each dataset. For each organism, the runtime was calculated as an average of all 200 genomes per batch. In general, the runtime depends on multiple factors, such as the specification and capabilities of the used computational platform. Since the runtime can vary depending on these various factors, the average statistics was used to show the central tendency of the runtime when comparing stringMLST vs. mlst. The runtime was calculated using the "date" command integrated in the Unix operating systems (e.g., *t=`date +%s`; mlst --legacy --scheme senterica --csv assembly.fasta > <output>; tt=`date +%s`; total_time=$((tt-t))*). For each

organism, the memory was calculated as the maximum memory recorded from all 200 genomes per batch, since all genomes were analyzed separately and concurrently. In the case of mlst, the recorded memory was the maximum memory of all the steps ran prior to mlst, such as trimming, *de novo* assembly, quality checking, filtering and ST typing. The memory used for these steps considerably varies from a few MBs to a few GBs (e.g., filtering vs. *de novo* assembly), and since the memory is a physical limitation of the computational platform, the maximum used memory was calculated for each organism and batch. The memory used was calculated using the "cgget" command that tracks various parameters from the Linux Control Groups (cgroups) per running job (e.g., *mlst --legacy --scheme senterica --csv assembly.fasta > <output>; r=`cgget -r memory.usage_in_bytes /slurm/uid_${UID}/job_${SLURM_JOBID}/`; mem=`echo $r | awk -F: '{print $3}'`*).

Incorporating stringMLST in ProkEvo

ProkEvo is a freely available and scalable computational platform capable of facilitating bacterial population genomics analyses while combining various independent algorithms in a portable pipeline [21]. One of the advantages of ProkEvo is its ability to facilitate the addition and removal of new steps and programs. For instance, more details about adding new program to ProkEvo are given here https://github.com/npavlovikj/ProkEvo/wiki/4.1.-Add-new-bioinformatics-tool-to-ProkEvo. By following these instructions, we were able to successfully add stringMLST to the current ProkEvo platform. The ultimate

432 description of how stringMLST was integrated into ProkEvo can be found here,
433 https://github.com/npavlovikj/MLST_stringMLST_analyses/tree/main/Prokevo_st
434 ringMLST.
435

436 Comparison between mlst and stringMLST performance
437 using ProkEvo

438 In order to compare the performance/accuracy of MLST and stringMLST as part
439 of the ProkEvo platform, two subsets of the *C. jejuni*, *L. monocytogenes*, *S.*
440 Typhimurium and *S. aureus* datasets used in this paper were selected. One subset
441 was composed of 100 randomly selected genomes, while the second one
442 contained 1,000. The subsets were randomly selected from the original isolates
443 used in this paper. As part of ProkEvo, stringMLST was run with the default kmer
444 length of 35. The ProkEvo workflows with mlst and stringMLST and the two
445 datasets were individually run on Crane - one of the high-performance computing
446 clusters at the Holland Computing Center. Once the four workflows finished, the
447 performance of ProkEvo with mlst and stringMLST and the datasets with 100 and
448 1,000 genomes, respectively, was compared using: i) the total running time; ii) the
449 percentage of non-classified STs; and iii) the percentage of agreement between
450 programs. Since ProkEvo is an automated platform, a list of NCBI-SRA
451 identifications was provided with the ProkEvo implementations with both mlst
452 and stringMLST. In brief, ProkEvo manages all the dependencies and
453 intermediate steps, and produces the final ST classification as an output.
454

455 **stringMLST-based kmer length optimization across**

456 **phylogenetic divergent bacterial pathogens**

457 In order to identify the optimal species-specific kmer length that minimizes the
458 frequency of ST miscalls, we ran stringMLST with a range of different kmer
459 lengths across phylogenetic divergent pathogenic species. First, we chose twenty-
460 three *S. enterica* serovars (*S*. Agona, *S*. Anatum, *S*. Braenderup, *S*. Derby, *S*.
461 Dublin, *S*. Enteritidis, *S*. Hadar, *S*. Heidelberg, *S*. Infantis, *S*. Javiana, *S*.
462 Johannesburg, *S*. Kentucky, *S*. Mbandaka, *S*. Montevideo, *S*. Muenchen, *S*.
463 Newport, *S*. Oranienburg, *S*. Poona, *S*. Saintpaul, *S*. Schwarzengrund, *S*.
464 Senftenberg, *S*. Thompson, *S*. Typhimurium), and for each dataset we randomly
465 selected 100 paired-end Illumina reads from NCBI-SRA. Second, for each dataset
466 we ran mlst and stringMLST with kmer lengths ranging from 20, 30, 35, 40, 45,
467 50, 55, 60, 65, 70, 80, 90. The kmer length of 10 was excluded due to its poor
468 performance in previous analyses. Additionally, we use data from fourteen
469 pathogens with Public Health relevance to widen the scope of the analysis and
470 assess the necessity of fine-tunning the kmer length on a more broadly selected
471 collection of species. In particular, we chose the following pathogens:
472 *Acinetobacter baumannii, Clostridioides difficile, Enterococcus faecium,*
473 *Escherichia coli, Haemophilus influenzae, Helicobacter pylori, Klebsiella*
474 *pneumoniae, Mycobacterium tuberculosis, Neisseria gonorrhoeae, Pseudomonas*
475 *aeruginosa, Streptococcus pneumoniae, Campylobacter jejuni, Listeria*
476 *monocytogenes, Staphylococcus aureus*. For each pathogen, we randomly selected
477 and downloaded 1,000 paired-end reads from NCBI-SRA and processed these

478 reads separately with mlst and stringMLST. stringMLST was run with kmer
479 lengths ranging from 20, 30, 35, 45, 55, 65, 70, 80, 90 and different schemes for
480 the different pathogens. Similarly to the *S. enterica* datasets, the kmer length of 10
481 was excluded from the analysis.

482 Across all datasets, the percentage of ST miscalls was calculated for
483 stringMLST for each kmer length, whereby miscalls were defined as "bad" ST
484 calls - calls with a missing or blank value. Next, for each dataset, the kmer length
485 that equated with the lowest percentage of ST miscalls was recorded. For some
486 datasets, multiple kmer lengths generated an identical lowest percentage for ST
487 miscalls. In this case, we applied a two-folded approach to select the most optimal
488 kmer length: 1) if kmer of length 35 was part of the kmer lengths that showed the
489 most optimal results, we recorded kmer 35 as the optimal kmer length since that is
490 the default and recommended value for stringMLST; or 2) if kmer of length 35
491 was not part of the kmer lengths that showed the most optimal results, we
492 recorded the kmer with the highest value as the most optimal one, since in general
493 our analysis showed that longer kmers consumed less computational resources
494 and speed up the entire analysis. Ultimately, the optimal kmer length and the
495 percentage of ST miscalls were visualized onto a core-genome phylogeny
496 generated for all twenty-three *S. enterica* serovars, as well as for all fourteen
497 pathogens including all twenty-three *S. enterica* serovars which jointly totaled
498 fifteen pathogens (total of 37 genomes, one per species including one per serovar
499 of *S. enterica*, were used to construct the core-genome phylogeny for
500 visualization purposes). The core-genome alignment was generated using Roary

with this set of parameters, "*roary -s -e --mafft -p 8 -cd 70 -i 70 ./prokka_output/*.gff -f roary_output*" (https://github.com/npavlovikj/MLST_stringMLST_analyses/blob/main/scripts/roary.submit).The phylogenetic tree was produced using FastTree [76] and visualized using iTOL [77], and the recorded statistics were extract with custom R scripts (https://github.com/npavlovikj/MLST_stringMLST_analyses/blob/main/figures_code/figures_code.Rmd).

In addition to calculating the percentage of ST miscalls for different kmer lengths with stringMLST, for each dataset we calculated the percentage of agreement (concordance) between mlst and stringMLST on ST calls ("good" or "bad"), as previously described here. Of note, when the stringMLST and mlst results were combined, the number of returned ST calls wasn't always 1,000 (the original size of the used datasets). If 1,000 reads are used with stringMLST, stringMLST generates ST calls for all 1,000 reads. On the other hand, when using mlst, a set of steps are used before mlst, including filtering, and a fraction of assemblies were disregarded due to poor quality. Thus, only genome sequences that passed through the mlst program and yielded a "good" or "bad" call were ultimately used to compare with stringMLST. The number of raw reads for each dataset, as well as the number of final reads from mlst used for these analyses are shown on S4 Table.

523 ## Statistical analyses

524 In order to compare the overall performance and accuracy of mlst vs. stringMLST
525 on ST-based classifications, the following statistics were used across all bacterial
526 species datasets: 1) ST richness; 2) Simpson's D index (1 – *D*) of diversity using
527 ST counts as input data; 3) Proportion of non-classified STs (missing values or
528 blank calls); and 4) Standard deviation of the proportion of non-classified STs.
529 These statistics were calculated to evaluate the algorithmic performance on ST-
530 based classification accuracy within and between bacterial species selected to be
531 used in the narrow scope analysis (*C. jejuni*, *S. aureus*, *L. monocytogenes*, and *S.*
532 *enterica*). ST richness was calculated by identifying the number of distinct STs
533 present in each species. The Simpson's D index of diversity (1- *D*) was used to
534 calculate the degree of genotypic diversity across species, using the diversity()
535 function available in the vegan (version 2.5-6) R library [29]. The proportion of
536 non-classified STs was calculated using the counts of isolates or genomes that
537 were not assigned a ST number after each run of either mlst or stringMLST. The
538 standard deviation of the proportion of non-classified STs was calculated using
539 the sd() function which is derived from an unbiased estimate of the sample
540 variance corrected by $n - 1$ (n for number of observations). The frequency of
541 genomes used for all analyses was calculated per batch and program across all
542 species, including across serovars for *S. enterica*. The relative frequency of the
543 most dominant ST lineages was also assessed across bacterial species.

544 PERMANOVA univariate or multivariate models were used to assess the
545 degree of association between the genome-intrinsic and –extrinsic factors with the

546 following dependent variables: ST richness, Simpson's D index of diversity, or
547 proportion of non-classified STs. Statistical models were built for each of the
548 dependent variables separately. Multivariate models included either the
549 combination of bacterial species and program, or serovars in the case of *S.*
550 *enterica* and program. These multivariate models were stated to calculate the
551 main and synergistic effects of the explanatory variables (e.g., species*program or
552 serovar*program). Univariate models were also assessed for each of the
553 dependent variables, using one of the following independent/explanatory
554 variables: 1) Genome-intrinsic variables: median number of contigs, mean of the
555 total count of nucleotides per genome, mean of the average GC% content per
556 genome, standard deviation of the number of contigs, standard deviation of the
557 total count of nucleotides per genome, and standard deviation of the average
558 GC% content per genome; 2) Genome-extrinsic variables: species, serovar of *S.*
559 *enterica*, program (mlst vs. stringMLST with kmer lengths of 10, 20, 30, 35, 45,
560 55, 65, 70, 80, 90), mean of the total count of unique STs per program, mean of
561 the total count of unique alleles across all genes per program, and the Simpson's
562 D index of diversity per species. Statistical significance and strength of
563 association between the dependent and independent variables were measured with
564 p-values ($p < 0.05$) and R-squared, respectively. In the case of contig size
565 (median), total number of nucleotides per genome (mean), and GC% content per
566 genome, summary statistic values (median or mean) were calculated grouped by
567 species and batch (there was a total of three batches per bacterial species or
568 serovar). For the total count of STs and total number of alleles in the database,

summary statistic values (mean) were calculated grouped by species, batch, and program. Lastly, the standard deviation of number of contigs, total count of nucleotides per genome, or GC% content per genome were calculated grouped by species. PERMANOVA models were run using the adonis() function with 1,000 permutations using the vegan (version 2.5-6) R library [29]. Principal component analysis (PCA) was used to analyze the dinucleotide distribution across species and across serovars for *S. enterica* with two dimensions using the prcomp() function. The PCA calculations and the selection of the number of PCs were done using the factoextra (version 1.0.7) library. Bar-plots, box-and-whiskers plots, and bivariate/trivariate scatter plots were used to assess the distribution and associations within and between dependent and independent/explanatory variables. The R software (version 4.0.3) and R libraries such as Tidyverse (version 1.3.0) were used to conduct all statistical analyses, and all R scripts are available here (https://github.com/npavlovikj/MLST_stringMLST_analyses/tree/main/figures_code). Data quality control was achieved with R base functions, in addition to the following packages: skimr (version 2.1.3) and visdat (version 0.5.3). Graphical visualizations were achieved using ggplot2 (version 3.3.2), GGally (version 2.1.2), and plotly (version 4.9.4.1). R code integrity was checked using the assertive (version 0.3-6) package.

590 # Results

591 The computational and analytical approaches used in this paper are shown on Fig
592 1. Our analytical approach was sub-divided into a narrow- and wide-scope
593 analysis aiming at accomplishing two goals: 1) Comparing the computational and
594 statistical performance of mlst vs. stringMLST; and 2) Optimizing the use of
595 stringMLST on a bacterial species basis and ultimately implementing it as part of
596 the ProkEvo computational genomics platform. First, we used freely available raw
597 Illumina paired-end sequence data from *C. jejuni*, *L. monocytogenes*, *S. enterica*
598 and *S. aureus*, to run stringMLST and mlst independently in order to compare the
599 accuracy in ST-based classifications and assess the computational needs and
600 performance in the overall analysis (narrow-scope step). In particular, for this
601 narrow-scope stage we performed a detailed comparative analysis between these
602 two programs including: i) analyses of computational performance and resources
603 needed (e.g., average runtime per genome and maximum memory needed to
604 analyze all genomes), and ii) statistical analyses to determine the accuracy of
605 classifications (e.g., ST richness, Simpson's D index of ST-based diversity,
606 proportion of miscalls, and percentage of agreement or concordance between
607 programs). For the wide-scope step, we systematically analyzed the accuracy and
608 concordance between mlst and stringMLST across a broad array of phylogenetic
609 divergent pathogens with direct implication for Public Health (*Acinetobacter*
610 *baumannii, Clostridioides difficile, Enterococcus faecium, Escherichia coli,*
611 *Haemophilus influenzae, Helicobacter pylori, Klebsiella pneumoniae,*
612 *Mycobacterium tuberculosis, Neisseria gonorrhoeae, Pseudomonas aeruginosa,*

613 *Streptococcus pneumoniae, Campylobacter jejuni, Listeria monocytogenes,*
614 *Salmonella enterica* and *Staphylococcus aureus*). Combined with the intra-species
615 analysis done across 23 serovars of *S. enterica*, our assessment aimed at revealing
616 the optimized kmer length to be used with stringMLST in order to: i) minimize
617 the percentage of ST miscalls, and ii) maximize the use of computational
618 resources by speeding up the analysis. Lastly, we provided an implementation of
619 stringMLST within ProkEvo - a freely available and scalable computational
620 platform that facilitates hierarchical genotyping of bacterial populations including
621 pan-genomic mapping [21].
622

623 Computational performance

624 The computational performance between stringMLST and mlst was measured
625 using two metrics: 1) The average computational runtime per genome; and 2) The
626 maximum memory used per dataset. The average runtime in minutes per genome
627 per batch between mlst and stringMLST with different kmer lengths, for *C. jejuni*,
628 *L. monocytogenes*, *S. aureus*, and *S.* Typhimurium (major representative of *S.*
629 *enterica*), is shown on Fig 2. While the runtime of mlst varies between 20 and 80
630 minutes per genome depending on the dataset used, all stringMLST runs with
631 different kmers finished within a few minutes (ranging from ~1-16 minutes when
632 kmer 10 was included and ~1-5 minutes when kmer 10 was excluded). Apart from
633 stringMLST with kmer 10, all other kmer lengths showed a uniform runtime. The
634 longer runtime observed with kmer 10 can be partially explained by the higher
635 number of kmers that were generated and used for mapping (S1 Fig). The

636 obtained results show that ST-based classifications are accomplished considerably
637 more rapidly when carried out using stringMLST compared to the standard MLST
638 program.

639 Additionally, a comparison of maximum memory used when both stringMLST
640 and mlst were run for *C. jejuni*, *L. monocytogenes*, *S. aureus*, and *S.* Typhimurium
641 (major representative of *S. enterica*) is shown on S2 Fig. Across all species, the
642 range of maximum memory usage for mlst and stringMLST (across all kmers)
643 was ~2-16GBs and ~3-30GBs respectively. Although the memory used across
644 datasets is variable, none of the analyses we ran exceeded 30GBs of RAM. Since
645 most high-performance computers can consistently provide resources from 32GBs
646 to a few TBs of RAM, the memory available should not be considered a
647 bottleneck for running either program.

648

649 Factors that can influence ST-based classification

650 First, we describe the characteristics and composition of the data utilized for
651 comparison between programs regarding ST-based classification in the narrow-
652 scope approach (utilization of fewer phylogenetic diverse pathogen datasets). The
653 frequency of genomes utilized per species and across programs is shown on S3A-
654 D Fig. The frequency of *S. enterica* genomes was higher than other species
655 because an equal sample of ~600 genomes was taken from 20 representative
656 zoonotic serovars (S4A-D Fig). An assessment of the proportion of the most
657 dominant STs across species (proportion ≥ 2% - S5A-D Fig) or serovars of *S.*
658 *enterica* (proportion ≥ 15% - S4N Fig) initially revealed a similar ST-based

659 distribution across programs. Furthermore, genome-intrinsic and -extrinsic factors
660 that could potentially impact the mlst vs. stringMLST algorithmic comparison and
661 performance were *a priori* determined and considered in the analysis. Among the
662 genome-intrinsic factors considered across species were the number of contigs per
663 genome (Fig 3A), the total number of nucleotides per genome (Fig 3B), GC%
664 content per genome (Fig 3C), and the distribution and composition of
665 dinucleotides per species (Fig 3D and S3E-F Fig). Similarly, the distribution of
666 the genome-intrinsic factors was analyzed across all twenty serovars of *S. enterica*
667 (S4G-L Fig). A correlogram (pairwise correlation analysis) was also used to
668 assess the bivariate correlation (Pearson's correlation coefficient) across genome-
669 intrinsic variables, for either all four bacterial species (S3G Fig) or serovars
670 across *S. enterica* (S4M Fig). At large, the differences observed in the distribution
671 of genomic-intrinsic variables were species driven, with a strong uniformity found
672 across serovars of *S. enterica*.
673 As for the genome-extrinsic variables, the total count of unique STs (for
674 species - Fig 3E) and unique number of alleles across all seven loci (for species -
675 Fig 3F), across all batches, were selected as factors that could influence the
676 comparative analysis between mlst and stringMLST. Similarly, the genome-
677 extrinsic variables were analyzed across all twenty serovars of *S. enterica* (S4E-F
678 Fig). Of note, database size differences (number of STs and alleles) may directly
679 influence the number of miscalls since it is expected that the larger the database
680 is, the more likely STs are to be classified, or to find a match, and not be
681 miscalled [30]. Considering the differences in genome-intrinsic and -extrinsic

682 variable distribution across species, such factors were further utilized for
683 assessing their statistical contribution in the accuracy of ST-based classification
684 between mlst vs. stringMLST.
685

686 Assessing the contribution of genome-intrinsic and –
687 extrinsic variables

688 In order to assess the statistical association and contribution of each genomic-
689 intrinsic and -extrinsic variable onto the accuracy of mlst vs. stringMLST on ST
690 calls (narrow-scope analysis since it only included four bacterial species, *C.*
691 *jejuni*, *S. aureus*, *L. monocytogenes*, and *S. enterica*), the following dependent
692 variables (outcomes) were used in the PERMANOVA models: 1) ST richness
693 (Fig 4A); 2) Simpson's D index of ST diversity (Fig 4B); and 3) Proportion of
694 non-classified STs (Fig 4C). Additionally, the standard deviation of the proportion
695 of non-classified STs was measured as an auxiliary metric for accuracy (Fig 4D).
696 At the species level, a multivariate model was used to examine the interaction of
697 species and program (mlst vs. stringMLST); whereas, the remaining analyses
698 were done using univariate models containing each genome-intrinsic and -
699 extrinsic variable for all three outcomes (S6A-L Fig, S7A-K Fig, S8A-L Fig).
700 For each variable, the significance and strength of association were assessed by
701 jointly examining the p-value ($p < 0.05$) and R-squared, respectively. For both ST
702 richness (Fig 4A) and the Simpson's D index of diversity (Fig 4B), the difference
703 between species explained the majority of the variation with ~98.3% and ~99%,
704 respectively. As expected, based on the phylogenetic divergence of the four

705 chosen pathogens, differences across species could largely be explained by
706 genome-intrinsic variables associated with genome composition, such as: GC%
707 content (p ~0.0009, R-squared ~44%) for ST richness, and the number of contigs
708 per genome (p ~0.0009, R-squared ~39.5%) for the Simpson's D index of
709 diversity (Fig 4A-B). Notably, for both ST richness and the Simpson's D index of
710 diversity most of the differences between species could be explained by variation
711 in genome composition (Fig 4A-B). Not surprisingly, co-linearity was observed
712 between ST richness and the Simpson's D index of diversity across species (Fig
713 4A). In the case of the proportion of non-classified STs (ST miscalls) (Fig 4C),
714 most of the variation was explained by inter-species differences (p ~0.0009, R-
715 squared ~33%), with the number of contigs per genome being the most important
716 genome-intrinsic contributing factor (p ~0.0009, R- squared ~27%). As for the
717 kmer length parameter used by stringMLST, results for ST richness and the
718 Simpson's D index of diversity were uniform across all lengths (Fig 4A-B).
719 However, when examining the proportion of miscalls (Fig 4C) and the standard
720 deviation of that proportion (Fig 4D), the data pointed toward the optimal kmer
721 length being between 35 and 65 across all four species (narrow-scope analysis).
722 Specifically, this kmer length range was defined based on two criteria: i)
723 minimization of the proportion of miscalls; and ii) less variation (standard
724 deviation) around the average of ST-based miscalls. Of note, mlst has the highest
725 proportion of miscalls and standard deviation of that proportion for both *L.*
726 *monocytogenes* and *C. jejuni* (Fig 4C-D), and the kmer length 10 for stringMLST
727 yielded very low accuracy and null results for ST richness and Simpson's D index

728 of diversity (Fig 4A-D). Differences between species across ST richness,
729 Simpson's D index of diversity, and proportion of ST miscalls along with all
730 genome-intrinsic and -extrinsic variables across programs (mlst vs. stringMLST)
731 were further examined here (Fig 5A-D, S9A-O Fig). Nonetheless, differences in
732 ST-based calls across programs were largely influenced by the bacterial species
733 dataset.

734 Given the complexity and diversity of the *S. enterica* population structure [12],
735 the stringMLST performance was analyzed across twenty zoonotic serovars
736 (S4O-R Fig), and resulted in a significant and predominant contribution of the
737 "serovar groupings" across all outcomes and PERMANOVA models (S10A-L
738 Fig, S11A-K Fig, S12A-L Fig): ST richness (p ~0.0009, R-squared ~75.4%),
739 Simpson's D index of diversity (p ~0.0009, R-squared ~88%), and proportion of
740 ST miscalls (p ~0.0009, R- squared ~35.4%). By assessing the distribution of the
741 model outcomes, along with PERMANOVA model results and bivariate
742 association between dependent and explanatory variables (S13A-R Fig), the
743 results recapitulated the species-level results with the optimal kmer length for
744 stringMLST being around 35 and 65, but also revealed the need to consider
745 difference across *S. enterica* serovars prior to implementation. Combined, these
746 accuracy-based results suggest that: i) stringMLST minimizes the ST miscalls
747 compared to mlst in a species-specific fashion, and by consequence the optimal
748 kmer length for stringMLST ranged from 35 to 65 overall; ii) the performance
749 and accuracy of stringMLST can vary across species and serovars of *S. enterica*
750 allowing for data-driven fine-tunning of the kmer length; and iii) the use of

751 sequence platform with longer reads which would maximize the number of
752 contigs per genome could directly alter both mlst and stringMLST accuracy in ST
753 calls across species.
754

755 Concordance between programs

756 Concordance between programs was calculated as the percentage of cases in
757 which outputs from both mlst vs. stringmlst agreed in the call ("good" or "bad").
758 Results demonstrating the percentage agreement in ST calls between mlst and
759 stringMLST with different kmer lengths are shown on Fig 6. With the exception
760 of kmer 10, across all species, the percentage of agreement between mlst and
761 stringMLST varies between 81.50% and 97.50%. In the case of *L.*
762 *monocytogenes*, *C. jejuni*, and *S. aureus*, the kmer length of 35 appears to be the
763 optimal value to reach the same accuracy as mlst, which matches the original
764 default and recommended parameter value for stringMLST [17]. However, for *S.*
765 *enterica* a higher percentage of agreement with MLST was achieved for kmer
766 lengths of 55 and 65 (Fig 6). This *S. enterica*-related observation recapitulated the
767 initial findings of decreased proportion of ST miscalls with higher kmer lengths
768 (Fig 4C). Of note, our finding collectively showed that the kmer length of 10
769 yielded low accuracy when compared to mlst and other stringMLST kmer lengths.
770 The most likely explanation for lower accuracy generated by kmer 10 is that
771 shorter kmers are more likely to map unambiguously onto a genome when
772 compared to other lengths. That high frequency of kmer length 10 on a given
773 dataset reflects their higher likelihood of mapping to multiple regions of a genome

774 (S1 Fig, S14A-B Fig). Overall, stringMLST is a rapidly deployable and
775 optimizable ST-based genotyping algorithm that in this narrow-scope analysis
776 proved to be applicable to four phylogenetic distinct pathogens.
777

778 Optimization of stringMLST kmer length across
779 phylogenetic divergent species

780 As previously proposed [17], the default kmer length for Illumina paired-end
781 reads for stringMLST is 35. However, our narrow-scope analysis across four
782 distinct pathogens (see above) suggested a species-specific variation in the
783 optimal kmer length capable of minimizing the proportion of ST miscalls.
784 Therefore, we systematically investigated what kmer length would give the fewest
785 ST miscalls (optimized length) with stringMLST across a diverse array of
786 phylogenetic divergent pathogens. Given our previous results, we first deepened
787 our investigation into the *S. enterica* population given the genetic and ecological
788 diversity across serovars. For that, we selected data from twenty-three *S. enterica*
789 zoonotic serovars and ran stringMLST with wide range of kmer lengths (20, 30,
790 35, 40, 45, 50, 55, 60, 65, 70, 80, 90). Fig 7A shows the core-genome phylogeny
791 mapping of the optimized kmer length across all twenty-three serovars along with
792 their corresponding percentage of ST miscalls. More detailed information on the
793 distribution of the percentage of ST miscalls for all used kmer lengths (20, 30, 35,
794 40, 45, 50, 55, 60, 65, 70, 80, 90) is shown on S15A Fig. As it can be seen on Fig
795 7A, many serovars (*S*. Anatum, *S*. Braenderup, *S*. Javiana, *S*. Mbandaka, *S*.
796 Montevideo, *S*. Oranienburg, *S*. Poona, *S*. Schwarzengrund, *S*. Senftenberg, *S*.

797 Typhimurium) have 0% of miscalls when the default kmer length 35 was used. *S*.
798 Infantis and *S*. Derby show the lowest percentage of ST miscalls (3% and 2%
799 respectively) with higher value of kmer, e.g., 90. Interestingly, *S*. Saintpaul
800 showed the highest percentage of ST miscalls when only considering the range of
801 kmer lengths used for the initial analyses (10-90). To investigate this further, we
802 ran stringMLST for *S*. Saintpaul with kmer lengths up to 240 (240 was chosen
803 because the maximum read length for the *S*. Saintpaul dataset is 250 base pairs or
804 nucleotides) (S15C-D Fig). As it can be seen on S15C Fig, the fewest ST miscalls
805 for *S*. Saintpaul were produced when kmer of length 140 was used (22%). When
806 comparing the percentage of ST miscalls between mlst and stringMLST, mlst
807 outperformed stringMLST for the used datasets and range of kmer lengths. In
808 addition to the percentage of ST miscalls, we calculated the percentage of ST
809 agreement between mlst and stringMLST with the range of kmer lengths (S15B
810 Fig). While for some serovars this percentage is the highest when kmer with
811 length 35 is used (e.g., *S*. Anatum, *S*. Braenderup, *S*. Javiana, *S*. Mbandaka, *S*.
812 Montevideo, *S*. Oranienburg, *S*. Poona, *S*. Schwarzengrund, *S*. Senftenberg, *S*.
813 Typhimurium), for other serovars (e.g., *S*. Derby, *S*. Dublin, *S*. Enteritidis, *S*.
814 Hadar, *S*. Heidelberg, *S*. Infantis, *S*. Kentucky, *S*. Saintpaul) the percentage of ST
815 agreement between the two programs was higher with higher kmer lengths.
816 In order to widen the scope of our phylogenetic-based analysis, we assessed the
817 percentage of ST miscalls across varying kmer lengths for divergent bacterial
818 pathogens with Public Health relevance. We selected 14 distinct organisms and
819 ran stringMLST with wide range of kmer lengths (20, 30, 35, 45, 55, 65, 70, 80,

820 90). Fig 7B depicts the core-genome phylogeny mapped results including the
821 optimal kmer length that minimized the percentage of ST miscalls. Of note, the
822 phylogeny contained fourteen distinct pathogens and twenty-three genomes across
823 each serovar of *S. enterica.* The distribution of the percentage of ST miscalls for
824 all used kmer lengths (20, 30, 35, 40, 45, 50, 55, 60, 65, 70, 80, 90) is shown on
825 S15E Fig. While the percentage of ST miscalls varied between 0% and 22%
826 across the *S. enterica* serovars as shown in Fig 7A, the percentage of miscalls is
827 more variable for the fourteen bacterial pathogens, ranging from 1.2% to 74.9%.
828 The datasets for *A. baumannii*, *C. jejuni*, *H. influenzae*, *K. pneumoniae*, *L.*
829 *monocytogenes*, *N. gonorrhoeae*, *S. aureus* and *S. pneumoniae* showed the lowest
830 percentage of ST calls with the default kmer length of 35. *C. difficile* and *M.*
831 *tuberculosis* had minimized ST miscalls with kmer lengths of 20 and 30
832 respectively, while *P. aeruginosa* with kmer length of 65. Interestingly, for *E.*
833 *faecium* and *H. pylori*, the optimal kmer lengths were 35 and 20, even though the
834 percentage of miscalls was high (74.9% and 67.6%). To further investigate this,
835 we ran stringMLST for *E. faecium* and *H. pylori* with kmer lengths up to 140 (140
836 was chosen because the maximum read length for the two datasets is 150 base
837 pairs or nucleotides) (S15G-H Fig, S15K-L Fig). As it can be seen on the Figures,
838 the percentage of miscalls was higher with higher kmer lengths, and the lower
839 kmer lengths yielded fewer miscalls, even though this number was still high.
840 Additionally, we ran stringMLST on another set of randomly selected 100 paired-
841 end reads for *E. faecium* (S15M-N Fig), *H. pylori* (S15I-J Fig) and *Enterococcus*
842 *faecalis* (S15O-P Fig). These 100 reads were not part of the initial datasets and

843 were chosen to validate that the initial random data selection was not completely
844 biased. We also added *E. faecalis* here due to its close phylogenetic association
845 with *E. faecium*. For *E. faecium* and *H. pylori* we observed the same pattern with
846 100 reads as with 1,000 reads. On the other hand, the pattern for *E. faecalis* was
847 quite opposite and as expected, with lowest percentage of ST miscalls of 5.43%
848 for kmer 35. When comparing the percentage of ST miscalls between mlst and
849 stringMLST, for some datasets, such as *H. pylori*, *C. jejuni*, *L. monocytogenes*, *M.*
850 *tuberculosis*, *N. gonorrhoeae*, *S. aureus*, mlst performed worse than stringMLST.
851 In addition to the percentage of ST miscalls, we calculated the percentage of ST
852 agreement between mlst and stringMLST with the range of kmer lengths (S15F
853 Fig). Of note, in the case of stringMLST, when the optimal kmer length was
854 above the default parameter of 35, the ultimately selected kmer length was picked
855 based on our empirical evidence for longer kmers being capable of speeding up
856 the computational analysis.
857 In summary, while the default kmer length of 35 used by stringMLST performs
858 accurately across many organisms, our systems-based approach that encompassed
859 the analysis of a variety of phylogenetic divergent organisms revealed: i) intra-
860 and inter-species variation in the percentage of ST miscalls requires fine-tunning
861 of the kmer length parameter; ii) lack of association between taxonomy or
862 phylogenetic placement of organisms and the optimal kmer length; and iii) unique
863 species behave as outliers for which stringMLST cannot be directly applied with
864 the default settings.
865

866 # Incorporating stringMLST in ProkEvo

867 ProkEvo was recently developed as an automated and scalable computational
868 platform for bacterial population genomics analyses that uses the Pegasus
869 Workflow Management System (WMS) [31] that allows for distributed use on
870 different computational platforms and rapid integration of novel programs [21]. In
871 particular, ProkEvo facilitates the use of a hierarchical approach for population
872 stratification with different layers of genotypic resolution. MLST-based
873 classification of genomes into STs is part of this hierarchical approach that has
874 been proven to be predictive of ecological traits such as AMR in *S. enterica*
875 lineages [57]. However, ProkEvo currently only uses the standard mlst algorithm
876 for ST calls [21]. As part of this paper, the stringMLST program was incorporated
877 into ProkEvo without any disruption in its workflow. The workflow design of
878 ProkEvo with both mlst and stringMLST is shown on S16 Fig.

879 In order to compare the performance of ProkEvo with mlst and stringMLST,
880 randomly shuffled subsets derived from the original datasets used for *C. jejuni*, *L.*
881 *monocytogenes*, *S.* Typhimurium, and *S. aureus* were used. One random subset
882 contained 100 genomes, while the second one had 1,000 genomes. ProkEvo was
883 run using either mlst or stringMLST on Crane, one of the high-performance
884 computing clusters at the Holland Computing Center [23]. For mlst, the pipeline
885 used was previously established and included a few required steps, such as quality
886 trimming and adapter clipping, *de novo* assembly and assembly discarding prior
887 to the ST mapping [21]. Based on the inter-species results shown here (Fig 6), the
888 default kmer length of 35 was used with stringMLST for this comparison. The

889 outcomes measured for this analysis were: i) total running time (Fig 8A); ii) the
890 percentage of non-classified STs (Fig 8B); and iii) the percentage of agreement
891 between programs (Fig 8C).

892 While the runtime of using ProkEvo with mlst varied from ~8 to 34 hours for
893 the subset containing 100 genomes, the runtime of ProkEvo with stringMLST
894 varied from ~25 minutes to 3 hours (Fig 8A). Similarly, for the larger datasets
895 containing 1,000 genomes, the runtime of ProkEvo with mlst varied from ~17 to
896 39 hours, while the runtime of ProkEvo with stringMLST varied from ~4 to 8
897 hours. Regardless of the pathogen species tested, stringMLST speeded up the
898 analyses ~4 times when utilizing 1,000 genomes across species.

899 In terms of accuracy in ST classifications, the use of stringMLST considerably
900 decreased the number of non-classified STs, regardless of the dataset size (100 or
901 1,000 genomes) and bacterial species (Fig 8B). In accordance, stringMLST
902 resulted in a higher frequency of genomes classified as novel STs (ST numbers
903 that were not classified by mlst) (S17 Fig). Additionally, the overall concordance
904 between mlst and stringMLST varies from 82% to 100% across all datasets. The
905 percentage of agreement is the lowest for *S.* Typhimurium, while it is the highest
906 for *S. aureus* (Fig 8C). The lower proportion of ST miscalls and high percentage
907 of agreement between programs for *S. aureus*, compared to other species, is
908 associated with its higher degree of genetic homogeneity (fewer dominant STs)
909 (S5 Fig). This difference in miscalls and concordance between programs may be
910 further explained by the variation in database sizes, since the PubMLST schemes

911 used for mlst have fewer alleles across all seven loci which results in fewer STs
912 compared to stringMLST as shown on S3 Table.
913 Previously, the scalability of ProkEvo was assessed by a comparative analysis
914 of its computational performance on Crane and OSG, using two datasets with
915 2,392 and 23,045 genomes each (10 X difference), and the standard mlst approach
916 for ST calling [21]. To further demonstrate the gain in computational runtime
917 obtained with the use of stringMLST within ProkEvo, the complete *S.*
918 Typhimurium dataset containing 23,045 genomes was run on OSG. While
919 ProkEvo with mlst finished all ST calls in 26 days and 6 hours when OSG was
920 used as a computational platform [21], ProkEvo with stringMLST completed the
921 task in 3 days and 6 hours. Altogether, stringMLST provides an accurate and
922 rapid alternative to mlst for scalable ST genotyping that is portable to be
923 implemented in any high-performance and high-throughput platform, with its use
924 being further facilitated by its implementation in ProkEvo.

925

926 # Discussion

927 The incorporation of WGS technology has advanced the study of bacterial
928 populations, since it has facilitated genotyping at different levels of resolution,
929 which in turn has proven to be predictive of, or associated with, inferable
930 ecological traits or epidemiological patterns [21] [32][33][34][35][36][37][38]. In
931 particular, the use of a hierarchical population structure analysis allows for
932 ancestral relationships and patterns of diversification to be inferred, while

933 determining the most important informative genotypic unit to be tracked over
934 time [21][39][40][41][12][42][43]. ST-based classification is an integral part of
935 the hierarchical genotyping approach [21][27]. ST lineages are formed based on
936 the utilization of allelic mapping across seven genome scattered loci that are
937 ubiquitously present across phylogenetic divergent bacterial species [8][9][44].
938 Such ST lineages can be further combined in clonal complexes, when sharing five
939 or more of the seven loci combinations - also called eBURST groups (eBG)
940 [10][45]. Thus, ST-based genotyping is widely used for a variety of reasons,
941 including: i) classification of genomes below the species level [8][9][44]; ii)
942 providing stable informative genotypic unit that can be used intra- and inter-
943 laboratory for mapping and tracking of populations [8][9][44]; iii) predictability
944 of ecological traits such as serovar in the case of *S. enterica*, and AMR across
945 bacterial species due to the linkage disequilibrium between MLST and accessory
946 loci [13][14][15][57]; and iv) inferring ancestral relationships through eBG
947 profiles [10][45]. ST-based genotyping is typically dependent on genome
948 assembly, which is efficient and accurate but not scalable and of rapid turn-
949 around [30][22]. However, stringMLST is a program capable of rapidly
950 classifying genomes into STs independently of genome assemblies [17]. Yet, a
951 systematic and scalable comparison between the standard MLST and stringMLST
952 programs is lacking [16]. Therefore, this study sought to comprehensively assess
953 the computational performance and accuracy of mlst vs. stringMLST across
954 phylogenetic divergent bacterial pathogens with direct implication for Public
955 Health. Additionally, this algorithmic comparison was designed to consider the

956 intra- and inter-species variation, in addition to the statistical contribution of
957 genome-intrinsic and -extrinsic factors on classification accuracy, aiming at
958 identifying actionable approaches that may be used to further optimize the
959 implementation of stringMLST.

960 Characterization of bacterial pathogens and performing molecular typing
961 provides valuable epidemiological information important for Public Health
962 agencies. There are multiple tools available for MLST classification, such as mlst
963 [22], ARIBA **Error! Reference source not found.**, stringMLST [17],
964 MentaLiST **Error! Reference source not found.**, STing **Error! Reference**
965 **source not found.**. In general, the available tools can be categorized based on the
966 input data they use - some tools use raw Illumina paired-end sequence data, while
967 others use *de novo* assemblies [16]. In order to generate the *de novo* assemblies, a
968 few pre-processing steps need to be performed, such as quality control, trimming,
969 assembly and filtering, that can be costly and require lots of computational
970 resources, such as memory and time. Using raw sequence data for ST-based
971 classification has a tremendous advantage especially in pathogen surveillance,
972 since all the costly steps prior to the *de novo* assembly are bypassed and the STs
973 calls are made as the sequence reads are generated. mlst uses *de novo* genome
974 assemblies as an input and performs mapping in order to align sequences to pre-
975 downloaded allelic files across all target loci. ARIBA identifies AMR-associated
976 genes, single nucleotide polymorphisms and ST calls using Illumina paired-end
977 raw sequencing reads. ARIBA clusters the raw reads by mapping them to genes,
978 and then performs local assembly within clusters to identify AMR genes and ST

calls. On the other hand, stringMLST and MentaLiST rely on kmer matching between raw sequence reads and available ST schemes that allows for fast mapping and ST-based typing. Both tools are shown to be accurate and fast for standard MLST classification, while providing comparable accuracy with MentaLiST albeit using less computational resources **Error! Reference source not found.**. STing is the successor of stringMLST - it uses the same algorithmic approach with additional computational applications for large MLST schemes such as ribosomal MLST (rMLST) and core-genome MLST (cgMLST) **Error! Reference source not found.**. All these tools have integrated ST schemes and/or provide utilities for downloading the available PubMLST databases. There are a few available comparisons of such tools for ST classification, mostly focusing on the computational resources used and the percentage of correctly classified STs [16]**Error! Reference source not found.Error! Reference source not found.**. When tools were tested with real outbreak datasets (*L. monocytogenes*, *E. coli*, *C. jejuni*, *S. enterica*) comprising 85 samples, stringMLST showed the fastest running time of 80.8 minutes and high accuracy in ST calls (100%) [16]. While MentaLiST does not scale well when reads with high coverage are used, it performs well on MLST schemes with up to a few thousand genes and alleles, such as cgMLST (~3,000 genes) **Error! Reference source not found.**. While most ST tools perform satisfactorily, there are some relevant bottlenecks to be considered. For example, some tools use out-of-date MLST databases that require manual curation, and can directly affect the accuracy of ST calls, especially when mixed and low coverage samples are used [16]. ST tools that are assembly and

1002 alignment free, such as stringMLST, STing and MentaLiST, show quite a few
1003 advantages in term of accuracy and efficiency that make them applicable for real-
1004 time molecular epidemiology and surveillance. Thus, we chose stringMLST as a
1005 representative of the kmer-based ST tools to perform a systems-based
1006 comparative analysis that assess the computational and statistical efficacy of ST
1007 calls across divergent pathogens in contrast to the legacy MLST approach.

1008 As shown here, the stringMLST accuracy can be affected by the species being
1009 tested without any specific phylogenetic patterns. In particular, the choice of kmer
1010 length used directly impacts the proportion of ST miscalls across species, and in
1011 certain cases it may not be applied as designed even after parameter tunning,
1012 which is likely a reflect of their varying population structure and pattern of
1013 genome diversification and architecture (e.g., horizontal gene transfer (HGT), and
1014 acquisition of mobile elements such as prophages and insertion sequences, etc.)
1015 [12][41][68][69][70][71][72][73]. A clear example is *S. enterica*, for which the
1016 accuracy of stringMLST varied across ecologically distinct serovars that are
1017 known to have unique pan-genomic composition as exemplified by their
1018 predictive prophage distribution [12][71][74][75]. To the best of our knowledge,
1019 the currently available comparisons between ST tools have not considered any
1020 systematic approach for parameter tunning across phylogenetic divergent
1021 species known to vary in population structure [21][27][67].

1022 In evaluating genome-intrinsic and -extrinsic variables that could contribute to
1023 differences in accuracy between mlst and stringMLST, it was found that the
1024 species level variation was mostly explained by the uniqueness of their genomic

1025 composition and number of contigs per genome. As genomic composition is an
1026 inheritable property of the bacterial species and reflects their evolutionary history
1027 and speciation patterns, this association with algorithmic performance was
1028 somewhat expected [46][47]. However, the contribution of the number of contigs
1029 making the overall difference between programs poses forth the hypothesis that
1030 by using sequencing platforms that generate longer reads, such as PacBio and
1031 Oxford Nanopore Technologies (ONT), both mlst and stringMLST accuracy in
1032 ST calls may be considerably altered in species-specific fashion, whereby
1033 accuracy would be expected to improve if HGT occurs at high rates. However,
1034 these sequencing technologies produce reads with lower accuracy (~80-90%) that
1035 may inflate the number of false allelic calls and consequently alter the distribution
1036 of STs - likely this would split major STs into sub-populations [48]**Error!**
1037 **Reference source not found.Error! Reference source not found.**. Therefore,
1038 while more work is needed in this field, current studies using hybrid assembly
1039 approaches of both Illumina short reads and ONT long reads **Error! Reference**
1040 **source not found.**, as well as only polished ONT reads **Error! Reference source**
1041 **not found.** for performing ST-based classification showed promising cost-
1042 effective results for this kind of molecular typing. Hence, we expect that
1043 stringMLST, or its successor STing, will be optimized for their implementation
1044 with longer read sequencing platform such as PacBio and Oxford Nanopore
1045 Technologies [14][49], which will in turn facilitate real-time surveillance of
1046 pathogens using hierarchical genotypes such as ST calls.

1047 While the kmer length of 35 is currently recommended as a default value of
1048 stringMLST, our systems-based approach demonstrated that for specific bacterial
1049 species it will result in increasing the frequency of ST miscalls which in turn may
1050 hinder epidemiological investigations. Across phylogenetic divergent pathogenic
1051 bacterial species, the optimal kmer length ranged from 20 to 140, regardless of
1052 their ancestral relationship or speciation pattern. The varying population structure,
1053 the pattern of genome diversification and architecture (e.g., impact of HGT), as
1054 well as sequence coverage may be some of the reasons underlying the observed
1055 statistics [12][41][68][69][70][71][72][73]. Although we hypothesize that longer
1056 sequence reads will help overcome this limitation, there is still a context-
1057 dependent consideration for parameter tunning and overall algorithmic
1058 implementation. Therefore, in the case of stringMLST, we suggest the following
1059 actionables to maximize its utilization, including: i) developers to consider
1060 implementing a pre-step that heuristically searches for the optimal kmer length
1061 (minimizes ST miscalls) in dataset-dependent fashion (sampling from the testing
1062 data), perhaps even by comparing with the standard MLST as positive controls;
1063 and/or ii) researchers to run wide range of kmer lengths on a subset of the dataset
1064 in order to select the optimal kmer length that minimizes the percentage of ST
1065 miscalls. Given the speed and scalability of stringMLST, using multiple kmer
1066 lengths is not likely to add much overhead to the analyses, and this provides an
1067 empirical statistical approach for kmer selection and optimization of ST
1068 classifications. With this data-driven fine-tunning of the kmer length, stringMLST

1069 is a powerful program that can be efficiently and effectively used in
1070 microbiological and epidemiological laboratories.
1071 We recently developed ProkEvo, a freely available scalable platform for
1072 performing hierarchical-based bacterial population genomics analyses [21].
1073 ProkEvo: 1) uses the Pegasus Workflow Management System to ensure
1074 reproducibility, scalability, and modularity; 2) uses high-performance and high-
1075 throughput computational platforms; 3) automates and scales multitude of
1076 computational analyses of a few to tens of thousands of bacterial genomes; 4) can
1077 run many thousands of analyses concurrently if the computational resources are
1078 available; 5) is easily modifiable and expandable platform that can incorporate
1079 additional algorithmic steps and custom scripts. The initial implementation of ST-
1080 based classifications through ProkEvo, as part of a hierarchical genotyping
1081 strategy to map and track populations, was done using the assembly-dependent
1082 MLST program [21][22]. Running mlst inside ProkEvo allows for parallelization
1083 of the genome assemblies (run per isolate or genome) which enhances scalability
1084 and facilitates the optimal use of computation resources. Theoretically, if there
1085 are *n* isolates and *n* cores available on the computational platform, ProkEvo can
1086 linearly utilize all resources and run all *n* independent tasks simultaneously.
1087 Typically, ST-based classifications are time consuming because the mapping
1088 process is run sequentially in a set of genomes instead of running them
1089 independently. Thus, using modular and distributed platforms such
1090 as ProkEvo for performing ST-based genotyping provides great benefit, especially
1091 if additional features such as other hierarchical genotypes and pan-genomic

1092 mapping tools are part of the same platform [21]. As part of this work, we
1093 modified ProkEvo to not only offer the standard assembly-dependent MLST
1094 mapping approach, but it now contains stringMLST, and our tests showed a
1095 significant speed-up in runtime for datasets ranging from a few hundreds to tens
1096 of thousands of genomes. To use ProkEvo with stringMLST, the researcher only
1097 needs to provide a list of SRA identifications and run the submit script without
1098 any advanced experience in high-performance or high-throughput computing.
1099 Depending on the configuration set, ProkEvo can use locally downloaded
1100 sequence data or download the data from NCBI directly. The Pegasus Workflow
1101 Managements System that is used by ProkEvo automatically handles the
1102 dependencies, as well as all the intermediate and final files. Thus, using platforms
1103 such as ProkEvo with fast tool for hierarchical genotyping, such as stringMLST,
1104 allows for robust and efficient population-based genomics analyses that facilitate:
1105 i) mapping and tracking of variants or lineages for epidemiological inquiries; ii)
1106 population structure analysis; and iii) ecological trait prediction using pan-
1107 genomic mapping to specific genotypes.
1108

1109 Conclusion

1110 In conclusion, stringMLST largely proved to be an accurate, rapid, and scalable
1111 tool for ST-based classifications that could be readily implemented in
1112 microbiological laboratories and epidemiological agencies. Notably, this
1113 comprehensive analysis of stringMLST across phylogenetic divergent bacterial
1114 pathogens, with varying degrees of clonality, revealed the potential for enhancing

its accuracy by parameter tunning (kmer length) in a dataset-dependent fashion. Specifically, we propose that the kmer length can be optimized in two ways on a case-by-case basis: 1) intrinsically by implementing a pre-step inside the algorithm to sample from the target data and select the optimal kmer length; or 2) by the user through a heuristic data mining approach to select the optimal kmer length prior to finalizing the ST calls. Also, by assessing genome-intrinsic and -extrinsic factors that could affect the stringMLST performance, our work suggests that longer sequence reads have the potential to improve its accuracy for specific bacterial species. Furthermore, the integration of stringMLST into ProkEvo allows users to take advantage of other hierarchical genotyping strategies, including pan-genomic mapping, which reproducibly facilitates ecological and epidemiological inquiries at scale. Ultimately, this work emphasizes the importance of developing robust algorithmic tools for mining WGS data that can have direct implications for mapping and tracking of bacterial populations.

Acknowledgements

This work was completed by utilizing the Holland Computing Center of the University of Nebraska, which receives support from the Nebraska Research Initiative, and using resources provided by the Open Science Grid, which is supported by the National Science Foundation and the U.S. Department of Energy's Office of Science. This research used the Pegasus Workflow Management Software funded by the National Science Foundation under grant #1664162. This publication made use of the PubMLST website

(https://pubmlst.org/) developed by Keith Jolley (Jolley & Maiden 2010, BMC Bioinformatics, 11:595) and sited at the University of Oxford. The development of that website was funded by the Wellcome Trust. We would like to greatly thank Mats Rynge for his extensive assistance and valuable suggestions while setting up and running ProkEvo on the Open Science Grid. We also thank Dr. Derek Weitzel and Karan Vahi for their technical support.

References

[1] Bedford J, Farrar J, Ihekweazu C, Kang G, Koopmans M, Nkengasong J. A new twenty-first century science for effective epidemic response. Nature. 2019 Nov;575(7781):130-6.

[2] Lewnard JA, Reingold AL. Emerging challenges and opportunities in infectious disease epidemiology. American journal of epidemiology. 2019 May 1;188(5):873-82.

[3] Armstrong GL, MacCannell DR, Taylor J, Carleton HA, Neuhaus EB, Bradbury RS, Posey JE, Gwinn M. Pathogen genomics in public health. New England Journal of Medicine. 2019 Dec 26;381(26):2569-80.

[4] Achtman M. How old are bacterial pathogens?. Proceedings of the Royal Society B: Biological Sciences. 2016 Aug 17;283(1836):20160990.

[5] Selander RK, Musser JM, Caugant DA, Gilmour MN, Whittam TS. Population genetics of pathogenic bacteria. Microbial pathogenesis. 1987 Jul 1;3(1):1-7.

1160 [6] Shapiro BJ. How clonal are bacteria over time?. Current opinion in
1161 microbiology. 2016 Jun 1;31:116-23.
1162 [7] Smith JM, Smith NH, O'Rourke M, Spratt BG. How clonal are bacteria?.
1163 Proceedings of the National Academy of Sciences. 1993 May
1164 15;90(10):4384-8.
1165 [8] Maiden MC, Bygraves JA, Feil E, Morelli G, Russell JE, Urwin R, Zhang
1166 Q, Zhou J, Zurth K, Caugant DA, Feavers IM. Multilocus sequence
1167 typing: a portable approach to the identification of clones within
1168 populations of pathogenic microorganisms. Proceedings of the National
1169 Academy of Sciences. 1998 Mar 17;95(6):3140-5.
1170 [9] Maiden MC. Multilocus sequence typing of bacteria. Annu. Rev.
1171 Microbiol.. 2006 Oct 13;60:561-88.
1172 [10] Feil EJ, Li BC, Aanensen DM, Hanage WP, Spratt BG. eBURST:
1173 inferring patterns of evolutionary descent among clusters of related
1174 bacterial genotypes from multilocus sequence typing data. Journal of
1175 bacteriology. 2004 Mar 1;186(5):1518-30.
1176 [11] Croucher NJ, Harris SR, Grad YH, Hanage WP. Bacterial genomes in
1177 epidemiology—present and future. Philosophical Transactions of the
1178 Royal Society B: Biological Sciences. 2013 Mar 19;368(1614):20120202.
1179 [12] Alikhan NF, Zhou Z, Sergeant MJ, Achtman M. A genomic overview of
1180 the population structure of Salmonella. PLoS genetics. 2018 Apr
1181 5;14(4):e1007261.

1182 [13] Achtman M, Wain J, Weill FX, Nair S, Zhou Z, Sangal V, Krauland MG,
1183 Hale JL, Harbottle H, Uesbeck A, Dougan G. Multilocus sequence typing
1184 as a replacement for serotyping in Salmonella enterica. PLoS Pathog. 2012
1185 Jun 21;8(6):e1002776.
1186 [14] Břinda K, Callendrello A, Ma KC, MacFadden DR, Charalampous T, Lee
1187 RS, Cowley L, Wadsworth CB, Grad YH, Kucherov G, O'Grady J. Rapid
1188 inference of antibiotic resistance and susceptibility by genomic neighbour
1189 typing. Nature microbiology. 2020 Mar;5(3):455-64.
1190 [15] MacFadden DR, Coburn B, Břinda K, Corbeil A, Daneman N, Fisman D,
1191 Lee RS, Lipsitch M, McGeer A, Melano RG, Mubareka S. Using genetic
1192 distance from archived samples for the prediction of antibiotic resistance
1193 in Escherichia coli. Antimicrobial agents and chemotherapy. 2020 Mar
1194 9;64(5):e02417-19.
1195 [16] Page AJ, Alikhan NF, Carleton HA, Seemann T, Keane JA, Katz LS.
1196 Comparison of classical multi-locus sequence typing software for next-
1197 generation sequencing data. Microbial genomics. 2017 Aug;3(8).
1198 [17] Gupta A, Jordan IK, Rishishwar L. stringMLST: a fast kmer based tool for
1199 multilocus sequence typing. Bioinformatics. 2017 Jan 1;33(1):119-21.
1200 [18] Abebe E, Gugsa G, Ahmed M. Review on major food-borne zoonotic
1201 bacterial pathogens. Journal of tropical medicine. 2020 Jun 29;2020.
1202 [19] Centers for Disease Control and Prevention. Foodborne germs and
1203 illnesses. Centers for Disease Control and Prevention. https://www. cdc.
1204 gov/foodsafety/foodborne-germs. html. 2016.

1205 [20] Centers for Disease Control and Prevention. Individual Salmonella
1206 serotypes reports. Centers for Disease Control and Prevention.
1207 https://www.cdc.gov/salmonella/reportspubs/salmonella-atlas/serotype-
1208 reports.html. 2020.
1209 [21] Pavlovikj N, Gomes-Neto JC, Deogun JS, Benson AK. ProkEvo: an
1210 automated, reproducible, and scalable framework for high-throughput
1211 bacterial population genomics analyses. PeerJ. 2021 May 21;9:e11376.
1212 [22] Seemann T, mlst Github https://github.com/tseemann/mlst.
1213 [23] HCC. 2008. Holland computing center | Nebraska.
1214 [24] Pordes R, Petravick D, Kramer B, Olson D, Livny M, Roy A, Avery P,
1215 Blackburn K, Wenaus T, Würthwein F+6 more. 2007. The open science
1216 grid. Journal of Physics: Conference Series 78:12057
1217 [25] Sfiligoi I, Bradley DC, Holzman B, Mhashilkar P, Padhi S, Wurthwein F.
1218 2009. The pilot way to grid resources using glideinWMS.
1219 [26] Anaconda. 2012. Anaconda | The World's Most Popular Data Science
1220 Platform.
1221 [27] Zhou Z, Alikhan NF, Mohamed K, Achtman M, Agama Study Group. The
1222 user's guide to comparative genomics with EnteroBase. Three case
1223 studies: micro-clades within Salmonella enterica serovar Agama, ancient
1224 and modern populations of Yersinia pestis, and core genomic diversity of
1225 all Escherichia. Biorxiv. 2019 Jan 1:613554.
1226 [28] Feil EJ, Cooper JE, Grundmann H, Robinson DA, Enright MC, Berendt T,
1227 Peacock SJ, Smith JM, Murphy M, Spratt BG, Moore CE. How clonal is

1228 Staphylococcus aureus?. Journal of bacteriology. 2003 Jun
1229 1;185(11):3307-16.
1230 [29] Oksanen J, Blanchet FG, Kindt R, Legendre P, Minchin PR, O'hara RB,
1231 Simpson GL, Solymos P, Stevens MH, Wagner H, Oksanen MJ. Package
1232 'vegan'. Community ecology package, version. 2013 Dec 12;2(9):1-295.
1233 [30] Jolley KA, Bray JE, Maiden MC. Open-access bacterial population
1234 genomics: BIGSdb software, the PubMLST. org website and their
1235 applications. Wellcome open research. 2018;3.
1236 [31] Deelman E, Singh G, Su MH, Blythe J, Gil Y, Kesselman C, Mehta G,
1237 Vahi K, Berriman GB, Good J, Laity A. Pegasus: A framework for
1238 mapping complex scientific workflows onto distributed systems. Scientific
1239 Programming. 2005 Jan 1;13(3):219-37.
1240 [32] Burnett E, Ishida M, De Janon S, Naushad S, Duceppe MO, Gao R,
1241 Jardim A, Chen JC, Tagg KA, Ogunremi D, Vinueza-Burgos C. Whole-
1242 genome sequencing reveals the presence of the blactx-m-65 gene in
1243 extended-spectrum β-lactamase-producing and multi-drug-resistant clones
1244 of salmonella serovar infantis isolated from broiler chicken environments
1245 in the Galapagos Islands. Antibiotics. 2021 Mar;10(3):267.
1246 [33] Cooper AL, Low AJ, Koziol AG, Thomas MC, Leclair D, Tamber S,
1247 Wong A, Blais BW, Carrillo CD. Systematic evaluation of whole genome
1248 sequence-based predictions of Salmonella serotype and antimicrobial
1249 resistance. Frontiers in microbiology. 2020 Apr 3;11:549.

1250 [34] Dallman TJ, Byrne L, Ashton PM, Cowley LA, Perry NT, Adak G,
1251 Petrovska L, Ellis RJ, Elson R, Underwood A, Green J. Whole-genome
1252 sequencing for national surveillance of Shiga toxin–producing Escherichia
1253 coli O157. Clinical Infectious Diseases. 2015 Aug 1;61(3):305-12.
1254 [35] Pightling AW, Pettengill JB, Luo Y, Baugher JD, Rand H, Strain E.
1255 Interpreting whole-genome sequence analyses of foodborne bacteria for
1256 regulatory applications and outbreak investigations. Frontiers in
1257 microbiology. 2018 Jul 10;9:1482.
1258 [36] Sheppard SK, Jolley KA, Maiden MC. A gene-by-gene approach to
1259 bacterial population genomics: whole genome MLST of Campylobacter.
1260 Genes. 2012 Jun;3(2):261-77.
1261 [37] Sheppard SK, Didelot X, Meric G, Torralbo A, Jolley KA, Kelly DJ,
1262 Bentley SD, Maiden MC, Parkhill J, Falush D. Genome-wide association
1263 study identifies vitamin B5 biosynthesis as a host specificity factor in
1264 Campylobacter. Proceedings of the national academy of sciences. 2013 Jul
1265 16;110(29):11923-7.
1266 [38] Alba P, Leekitcharoenphon P, Carfora V, Amoruso R, Cordaro G, Di
1267 Matteo P, Ianzano A, Iurescia M, Diaconu EL, Pedersen SK, Guerra B.
1268 Molecular epidemiology of Salmonella Infantis in Europe: insights into
1269 the success of the bacterial host and its parasitic pESI-like megaplasmid.
1270 Microbial genomics. 2020 May;6(5).

1271 [39] Cheng L, Connor TR, Sirén J, Aanensen DM, Corander J. Hierarchical
1272 and spatially explicit clustering of DNA sequences with BAPS software.
1273 Molecular biology and evolution. 2013 Feb 13;30(5):1224-8.
1274 [40] Tonkin-Hill G, Lees JA, Bentley SD, Frost SD, Corander J. Fast
1275 hierarchical Bayesian analysis of population structure. Nucleic Acids
1276 Research. 2019 Jun 20;47(11):5539-49.
1277 [41] Didelot X, Bowden R, Street T, Golubchik T, Spencer C, McVean G,
1278 Sangal V, Anjum MF, Achtman M, Falush D, Donnelly P. Recombination
1279 and population structure in Salmonella enterica. PLoS genetics. 2011 Jul
1280 28;7(7):e1002191.
1281 [42] Gymoese P, Kiil K, Torpdahl M, Østerlund MT, Sørensen G, Olsen JE,
1282 Nielsen EM, Litrup E. WGS based study of the population structure of
1283 Salmonella enterica serovar Infantis. BMC genomics. 2019 Dec;20(1):1-1.
1284 [43] Liao J, Orsi RH, Carroll LM, Wiedmann M. Comparative genomics
1285 reveals different population structures associated with host and geographic
1286 origin in antimicrobial-resistant Salmonella enterica. Environmental
1287 microbiology. 2020 Jul;22(7):2811-28.
1288 [44] Maiden MC, Van Rensburg MJ, Bray JE, Earle SG, Ford SA, Jolley KA,
1289 McCarthy ND. MLST revisited: the gene-by-gene approach to bacterial
1290 genomics. Nature Reviews Microbiology. 2013 Oct;11(10):728-36.
1291 [45] Spratt BG, Hanage WP, Li B, Aanensen DM, Feil EJ. Displaying the
1292 relatedness among isolates of bacterial species–the eBURST approach.
1293 FEMS microbiology letters. 2004 Dec 1;241(2):129-34.

1294 [46] Bobay LM, Ochman H. Impact of recombination on the base composition
1295 of bacteria and archaea. Molecular biology and evolution. 2017 Oct
1296 1;34(10):2627-36.
1297 [47] Raghavan R, Kelkar YD, Ochman H. A selective force favoring increased
1298 G+ C content in bacterial genes. Proceedings of the National Academy of
1299 Sciences. 2012 Sep 4;109(36):14504-7.
1300 [48] De Maio N, Shaw LP, Hubbard A, George S, Sanderson ND, Swann J,
1301 Wick R, AbuOun M, Stubberfield E, Hoosdally SJ, Crook DW.
1302 Comparison of long-read sequencing technologies in the hybrid assembly
1303 of complex bacterial genomes. Microbial genomics. 2019 Sep;5(9).
1304 [49] Page AJ, Keane JA. Rapid multi-locus sequence typing direct from
1305 uncorrected long reads using Krocus. PeerJ. 2018 Jul 31;6:e5233.
1306 [50] Bolger AM, Lohse M, Usadel B. Trimmomatic: a flexible trimmer for
1307 Illumina sequence data. Bioinformatics. 2014 Aug 1;30(15):2114-20.
1308 [51] Andrews S. FASTQC: a quality control tool for high throughput sequence
1309 data. Available at
1310 http://www.bioinformatics.babraham.ac.uk/projects/fastqc/. 2010.
1311 [52] Bankevich A, Nurk S, Antipov D, Gurevich AA, Dvorkin M, Kulikov AS,
1312 Lesin VM, Nikolenko SI, Pham S, Prjibelski AD, Pyshkin AV. SPAdes: a
1313 new genome assembly algorithm and its applications to single-cell
1314 sequencing. Journal of computational biology. 2012 May 1;19(5):455-77.
1315 [53] Gurevich A, Saveliev V, Vyahhi N, Tesler G. QUAST: quality assessment
1316 tool for genome assemblies. Bioinformatics. 2013 Apr 15;29(8):1072-5.

1317 [54] Treangen TJ, Sommer DD, Angly FE, Koren S, Pop M. Next generation
1318 sequence assembly with AMOS. Current Protocols in Bioinformatics.
1319 2011 Mar;33(1):11-8.
1320 [55] Rice P, Longden I, Bleasby A. EMBOSS: the European molecular biology
1321 open software suite. Trends in genetics. 2000 Jun 1;16(6):276-7.
1322 [56] Rizk G, Lavenier D, Chikhi R. DSK: k-mer counting with very low
1323 memory usage. Bioinformatics. 2013 Mar 1;29(5):652-3.
1324 [57] Gomes-Neto JC, Pavlovikj N, Cano C, Abdalhamid B, Al-Ghalith GA,
1325 Loy JD, Knights D, Iwen PC, Chaves BD, Benson AK. Heuristic and
1326 hierarchical-based population mining of Salmonella enterica lineage I pan-
1327 genomes as a platform to enhance food safety. Front. Sustain. Food Syst.
1328 5:725791. doi: 10.3389/fsufs.2021.725791.
1329 [58] Valieris R. Parallel-fastq-dump. GitHub. Available at
1330 https://github.com/rvalieris/parallelfastq-dump. 2020.
1331 [59] Rang FJ, Kloosterman WP, de Ridder J. From squiggle to basepair:
1332 computational approaches for improving nanopore sequencing read
1333 accuracy. Genome biology. 2018 Dec;19(1):1-1.
1334 [60] Rhoads A, Au KF. PacBio sequencing and its applications. Genomics,
1335 proteomics & bioinformatics. 2015 Oct 1;13(5):278-89.
1336 [61] Chen Z, Erickson DL, Meng J. Benchmarking hybrid assembly
1337 approaches for genomic analyses of bacterial pathogens using Illumina
1338 and Oxford Nanopore sequencing. BMC genomics. 2020 Dec;21(1):1-21.

1339 [62] Liou CH, Wu HC, Liao YC, Lauderdale TL, Huang IW, Chen FJ.
1340 nanoMLST: accurate multilocus sequence typing using Oxford Nanopore
1341 Technologies MinION with a dual-barcode approach to multiplex large
1342 numbers of samples. Microbial genomics. 2020 Mar;6(3).
1343 [63] Feijao P, Yao HT, Fornika D, Gardy J, Hsiao W, Chauve C, Chindelevitch
1344 L. MentaLiST–A fast MLST caller for large MLST schemes. Microbial
1345 genomics. 2018 Feb;4(2).
1346 [64] Espitia-Navarro HF, Chande AT, Nagar SD, Smith H, Jordan IK,
1347 Rishishwar L. STing: accurate and ultrafast genomic profiling with exact
1348 sequence matches. Nucleic acids research. 2020 Aug 20;48(14):7681-9.
1349 [65] Hunt M, Mather AE, Sánchez-Busó L, Page AJ, Parkhill J, Keane JA,
1350 Harris SR. ARIBA: rapid antimicrobial resistance genotyping directly
1351 from sequencing reads. Microbial genomics. 2017 Oct;3(10).
1352 [66] Page AJ, Cummins CA, Hunt M, Wong VK, Reuter S, Holden MT,
1353 Fookes M, Falush D, Keane JA, Parkhill J. Roary: rapid large-scale
1354 prokaryote pan genome analysis. Bioinformatics. 2015 Nov
1355 15;31(22):3691-3.
1356 [67] Zhou Z, Alikhan NF, Mohamed K, Fan Y, Achtman M, Brown D,
1357 Chattaway M, Dallman T, Delahay R, Kornschober C, Pietzka A. The
1358 EnteroBase user's guide, with case studies on Salmonella transmissions,
1359 Yersinia pestis phylogeny, and Escherichia core genomic diversity.
1360 Genome research. 2020 Jan 1;30(1):138-52.

1361 [68] Sheppard SK, Colles FM, McCARTHY ND, Strachan NJ, Ogden ID,
1362 Forbes KJ, Dallas JF, Maiden MC. Niche segregation and genetic
1363 structure of Campylobacter jejuni populations from wild and agricultural
1364 host species. Molecular ecology. 2011 Aug;20(16):3484-90.
1365 [69] Sheppard SK, Cheng L, Méric G, De Haan CP, Llarena AK, Marttinen P,
1366 Vidal A, Ridley A, Clifton-Hadley F, Connor TR, Strachan NJ. Cryptic
1367 ecology among host generalist Campylobacter jejuni in domestic animals.
1368 Molecular ecology. 2014 May;23(10):2442-51.
1369 [70] Yahara K, Didelot X, Ansari MA, Sheppard SK, Falush D. Efficient
1370 inference of recombination hot regions in bacterial genomes. Molecular
1371 biology and evolution. 2014 Jun 1;31(6):1593-605.
1372 [71] Mottawea W, Duceppe MO, Dupras AA, Usongo V, Jeukens J, Freschi L,
1373 Emond-Rheault JG, Hamel J, Kukavica-Ibrulj I, Boyle B, Gill A.
1374 Salmonella enterica prophage sequence profiles reflect genome diversity
1375 and can be used for high discrimination subtyping. Frontiers in
1376 microbiology. 2018 May 4;9:836.
1377 [72] den Bakker HC, Desjardins CA, Griggs AD, Peters JE, Zeng Q, Young
1378 SK, Kodira CD, Yandava C, Hepburn TA, Haas BJ, Birren BW.
1379 Evolutionary dynamics of the accessory genome of Listeria
1380 monocytogenes. PLoS One. 2013 Jun 25;8(6):e67511.
1381 [73] Castillo-Ramírez S, Corander J, Marttinen P, Aldeljawi M, Hanage WP,
1382 Westh H, Boye K, Gulay Z, Bentley SD, Parkhill J, Holden MT.
1383 Phylogeographic variation in recombination rates within a global clone of

1384 methicillin-resistant Staphylococcus aureus. Genome biology. 2012
1385 Dec;13(12):1-3.
1386 [74] Laing CR, Whiteside MD, Gannon VP. Pan-genome analyses of the
1387 species Salmonella enterica, and identification of genomic markers
1388 predictive for species, subspecies, and serovar. Frontiers in microbiology.
1389 2017 Jul 31;8:1345.
1390 [75] Ferrari RG, Rosario DK, Cunha-Neto A, Mano SB, Figueiredo EE, Conte-
1391 Junior CA. Worldwide epidemiology of Salmonella serovars in animal-
1392 based foods: a meta-analysis. Applied and environmental microbiology.
1393 2019 Jul 1;85(14):e00591-19.
1394 [76] Price MN, Dehal PS, Arkin AP. FastTree: computing large minimum
1395 evolution trees with profiles instead of a distance matrix. Molecular
1396 biology and evolution. 2009 Jul 1;26(7):1641-50.
1397 [77] Letunic I, Bork P. Interactive Tree Of Life (iTOL) v5: an online tool for
1398 phylogenetic tree display and annotation. Nucleic acids research. 2021 Jul
1399 2;49(W1):W293-6.

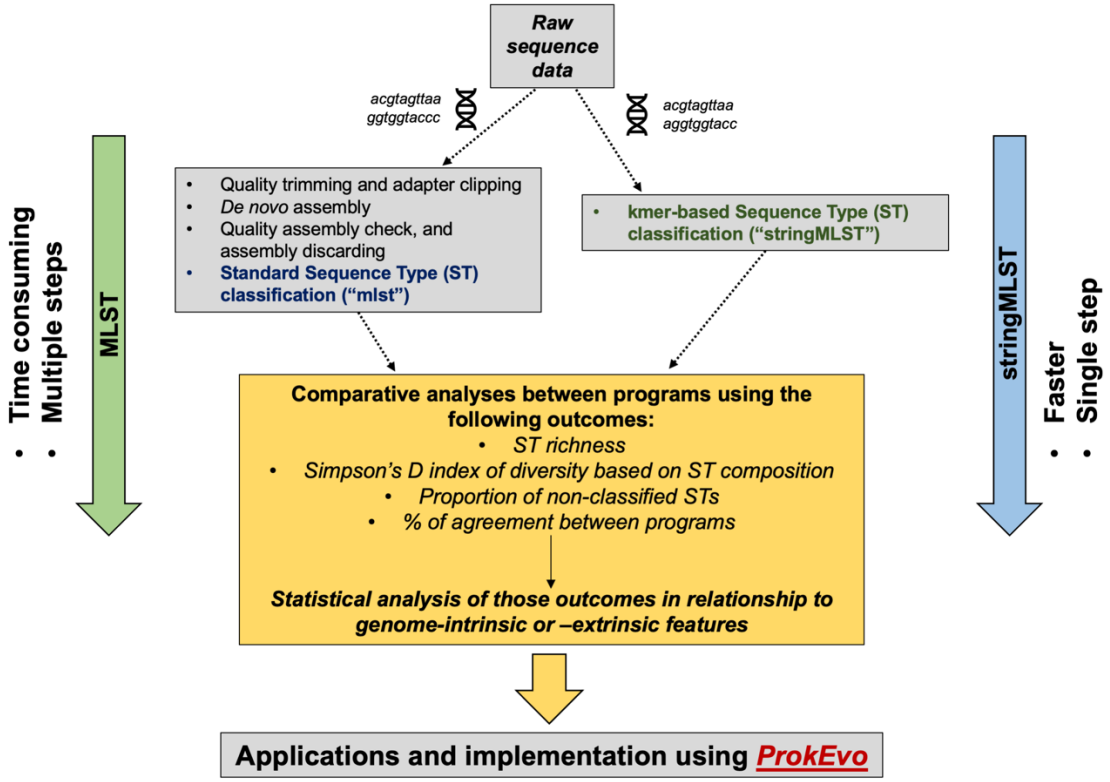

Figure 1. Computational workflow describing the analytical steps for a comparative analysis of two algorithms used for ST-based classification.
From top-down, the first step (narrow-scope) of the analytical approach entailed the acquisition and processing of Illumina paired-end raw reads from four distinct pathogens (*C. jejuni*, *L. monocytogenes*, *S. enterica* and *S. aureus*), through an assembly-dependent (mlst) or assembly-free (stringMLST) approach for ST-based classification. Next, a set of comparative analyses encompassing measuring the computational performance, statistical metrics, and modeling were used to assess the accuracy and efficiency of mlst vs. stringMLST. Additionally, the contribution of genome-intrinsic and –extrinsic variables were used to identify explanatory factors that could impact the algorithmic efficiency across phylogenetic divergent species. Upon identification of inter-species differences in the performance of stringMLST, a wide-scope analysis was done to assess its accuracy across an array of other fourteen phylogenetic divergent pathogenic species of bacteria with Public Health relevance. Ultimately, stringMLST was added to the computational platform ProkEvo to facilitate ST-based classification at scale, as part of a hierarchical-based approach for population genomic analyses.

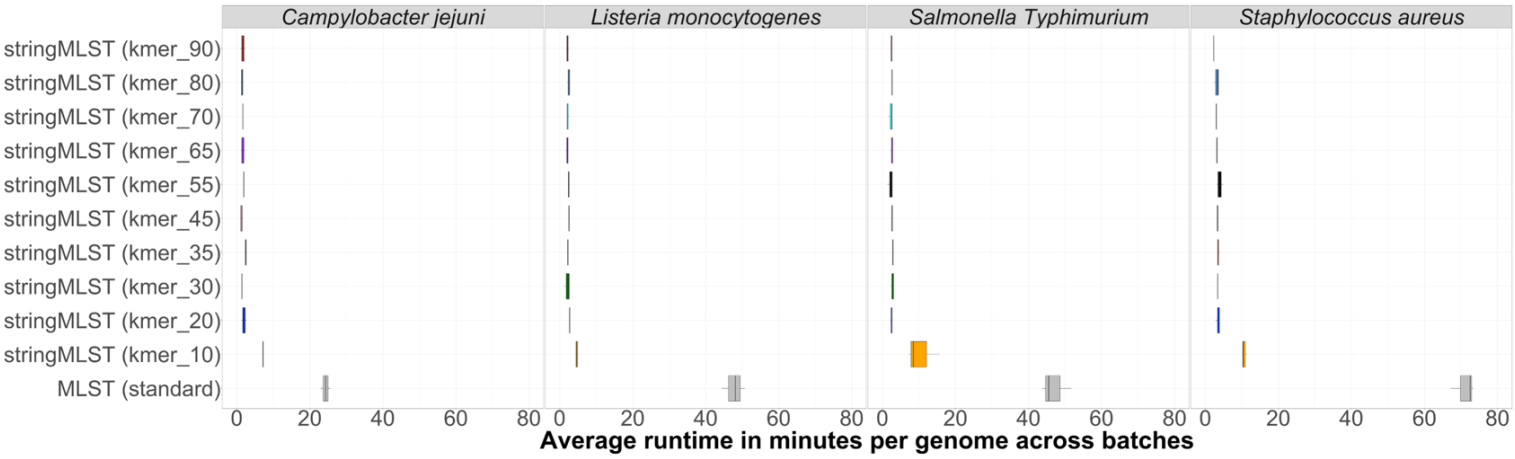

Figure 2. Box-and-whiskers plot showing the comparison of the average runtime per genome per batch (in minutes) needed by mlst and stringMLST for ST classification of genomes across four distinct bacterial species.
In order to compare the average runtime used by mlst and stringMLST with different kmer values, we chose four different datasets, including four phylogenetic divergent bacterial pathogenic species: *C. jejuni*, *L. monocytogenes*, one major serovar of *S. enterica* (*S.* Typhimurium) and *S. aureus* - using 600 randomly selected genomes for each species. These 600 genomes were randomly split into three batches with 200 genomes each. We then ran mlst with all required steps, such as quality trimming and adapter clipping, *de novo* assembly and assembly discarding, on each batch and dataset. Separately, we ran stringMLST with a range of 10 different kmer values (10, 20, 30, 35, 45, 55, 65, 70, 80, 90) on each dataset, including the default length of 35 (y-axis). For each organism, the runtime was calculated as an average of 200 genomes per batch - since there were three batches, three datapoints were used to depict the distribution of runtime in minutes (x-axis).

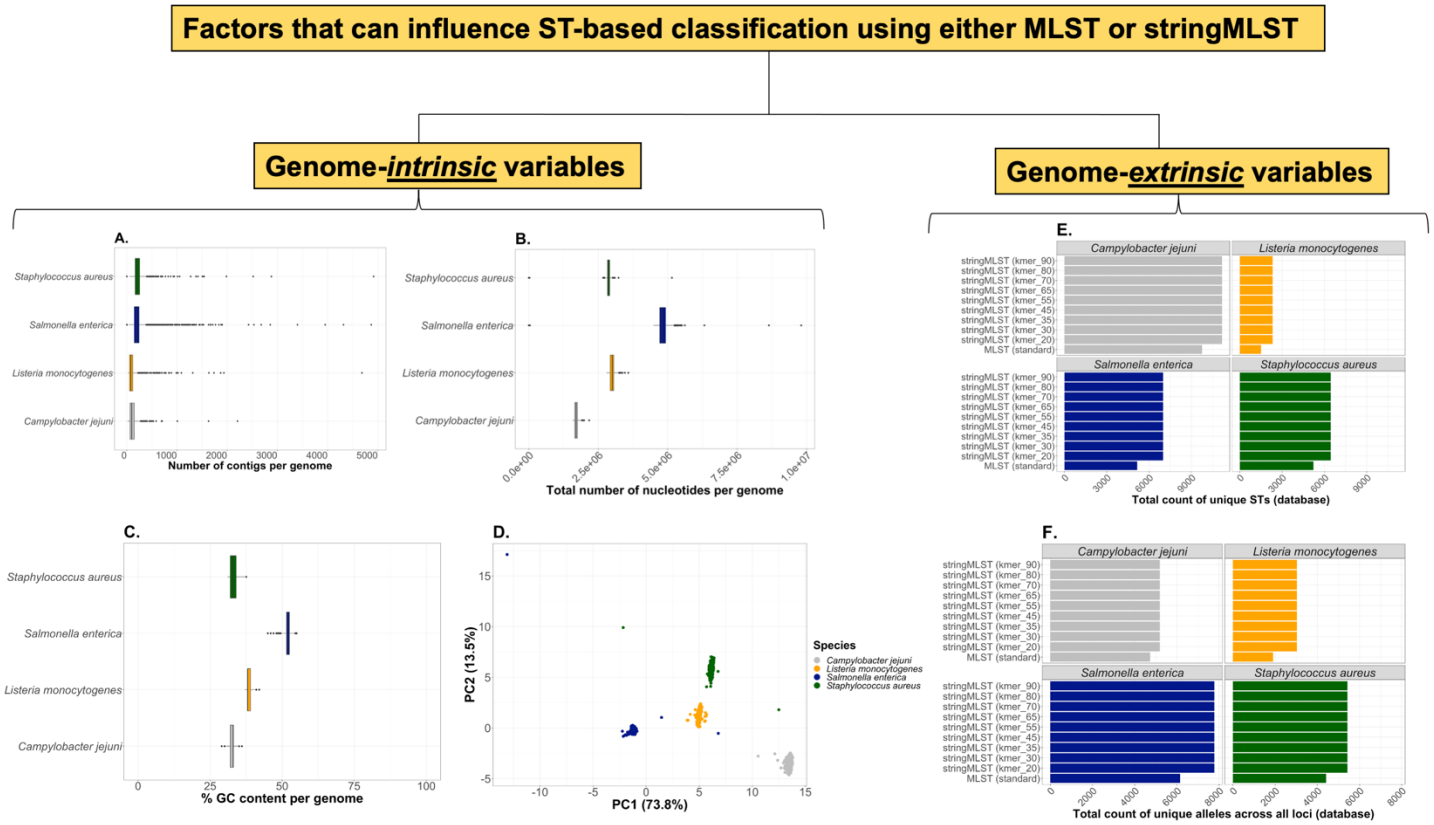

Figure 3. Genome-intrinsic and –extrinsic variables that can impact the accuracy of ST-based classification using either mlst (MLST-based genotyping) or stringMLST algorithmic approaches.
Box-and-whiskers plot showing genome-intrinsic variables, varying in distribution according to the bacterial species (A-C as y-axis), that may affect ST-based classification, include: (A) Number of contigs per genome (x-axis); (B) Total number of nucleotides per genome (x-axis); (C) GC% content per genome (x-axis); and (D) Dinucleotide composition of genomes. (D) Inter-species PCA using the relative frequency of all pairs of dinucleotides (16 pairs) present in the genome as input data. Only two PCs are shown, and the percentage of variance explained by either PC is depicted in parenthesis. Bar plots showing genome-extrinsic variables that may influence the performance of mlst vs. stringMLST across species include but are not limited to: (E) Total count of unique STs per database (ST richness in the database used for mapping of raw reads or assemblies) (x-axis); and (F) Total count of unique alleles across all seven loci used for ST classification (x-axis). Specifically, the differences in ST richness and allelic composition in the databases reflect difference between mlst vs. stringMLST, and were not impacted by the kmer length (E-F, y-axis).

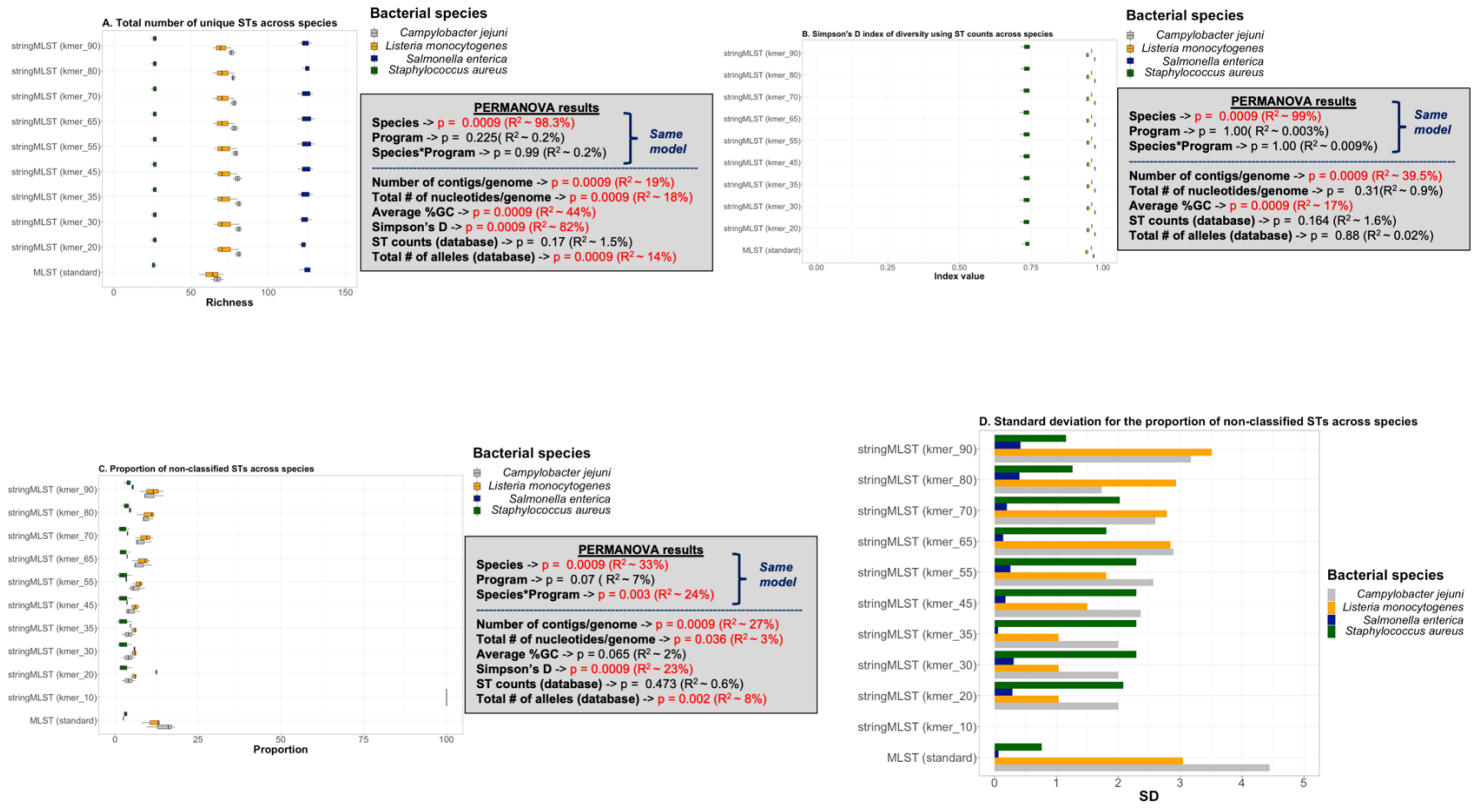

Figure 4. Statistical analysis of ST-based classification outcomes for comparison between mlst and stringMLST performance across bacterial species.
(A-C) Box-and-whiskers plots A-C demonstrate the relationship between ST richness (x-axis), Simpson's index of diversity (1 – *D*) based on ST composition (x-axis), or the proportion of non-classified STs (x-axis) across bacterial species (color-coded differently) and programs (y-axis), respectively. Along with plots A-C are depicted all PERMANOVA results including *p*-values ($p < 0.05$) and the univariate or synergistic contribution of factors measured by *R*-squared. PERMANOVA modeling was done in two specific ways: 1) A model including species, program, and their interaction, considering that those were the main variables of interest; and 2) All other results were calculated using univariate models and included modeling using genome-intrinsic (number of contigs per genome, total number of nucleotides per genome, and average GC% content) and –extrinsic (Simpson's D index of diversity, ST and allelic counts per database) variables. (D) Bar plot depicting the distribution of the standard deviation (SD, y-axis) for the proportion of non-classified STs based on species (color-coded differently) and programs (y-axis).

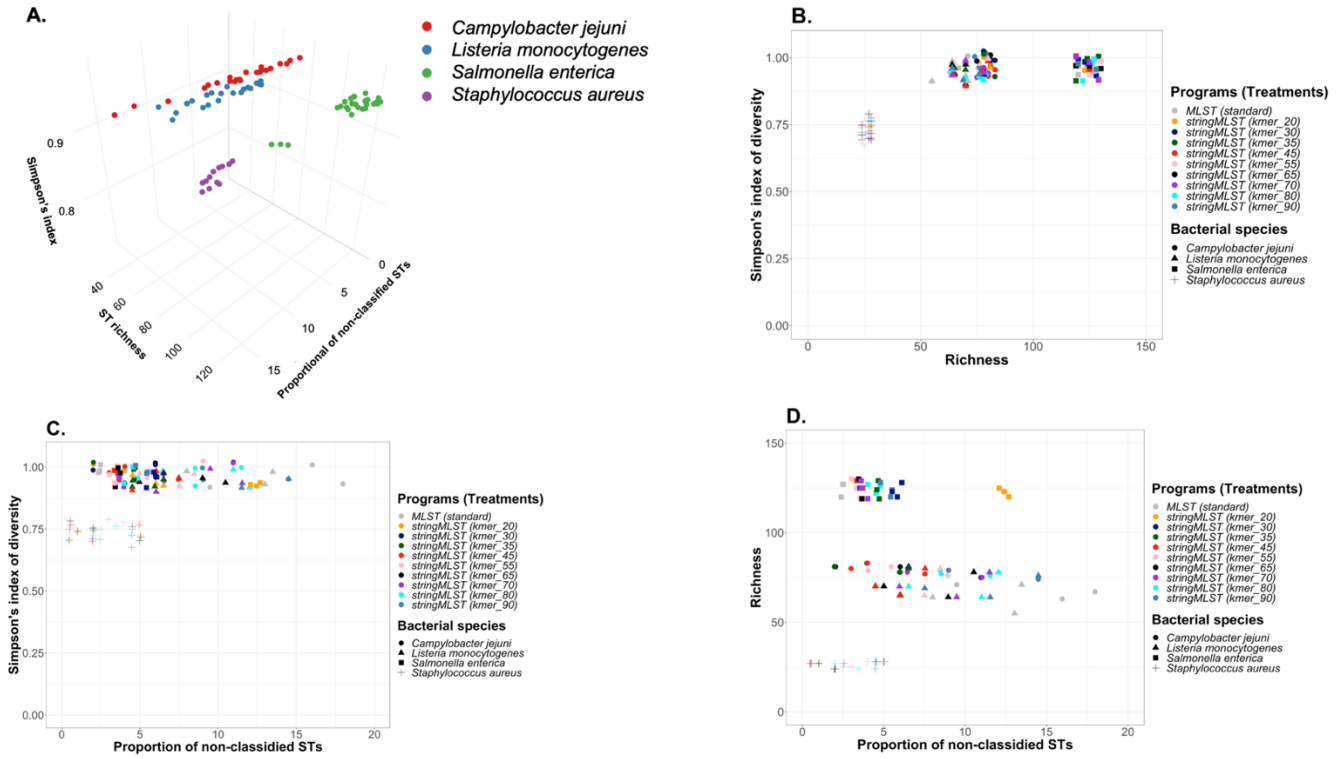

Figure 5. Multi-dimensional analysis of ST-based classification outcomes across different species using mlst vs. stringMLST.
(A) Tri-dimensional scatter plot demonstrating species grouping based on the outcomes calculated using the ST classification across programs, including: 1) Simpson's index of diversity (1 – *D,* Simpson's index); 2) ST richness; and 3) proportion of non-classified STs. (B-D) Biplots demonstrating groupings formed across species and programs based on the same outcomes. Scatter plot B depicts groupings produced based on the relationship between Simpson's index of diversity vs. ST richness (Richness); whereas scatter plot C shows the relationship between the Simpson's index of diversity and the proportion of non-classified STs; and lastly, scatter plot D depicts the relationship between ST richness (Richness) and the proportion of non-classified STs.

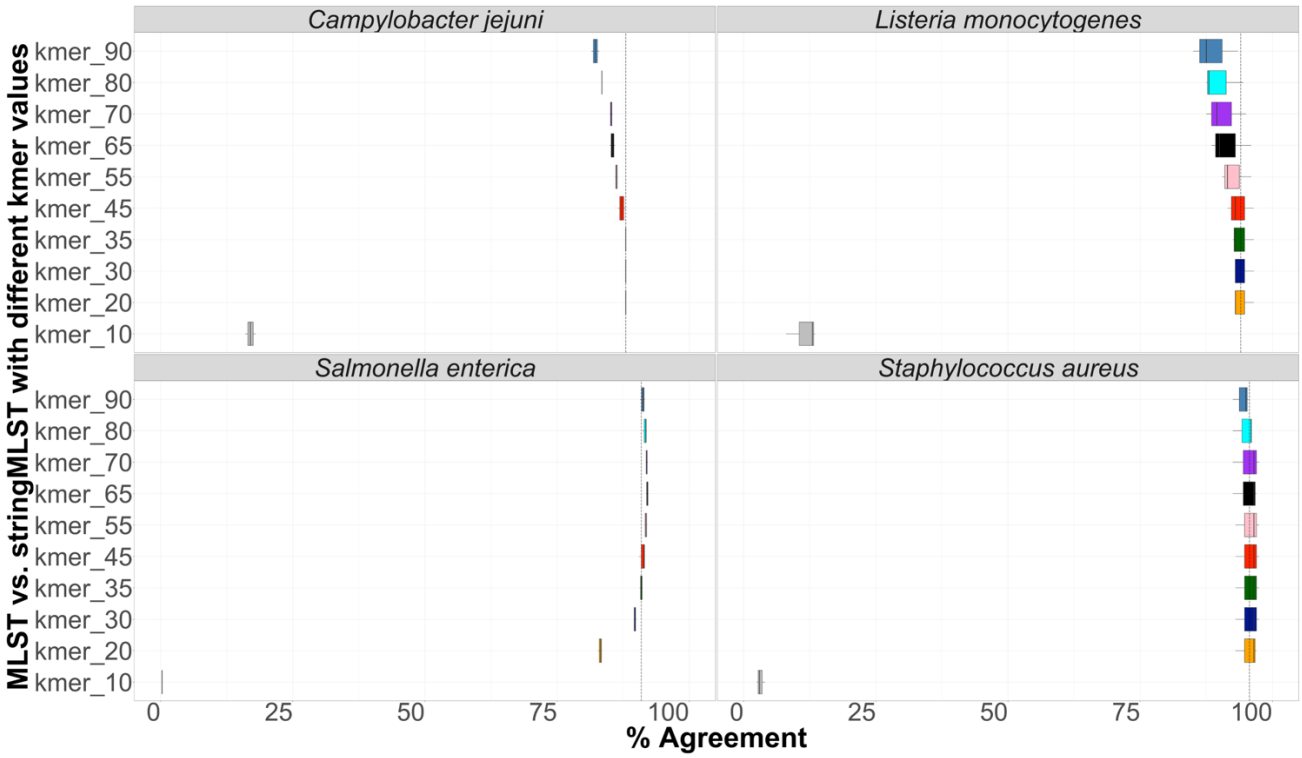

Figure 6. Box-and-whiskers plot depicting the concordance between mlst and stringMLST in ST calls.
Four different datasets belonging to four phylogenetic distinct bacterial pathogens, including *C. jejuni* (600 genomes), *L. monocytogenes* (600 genomes), *S. enterica* (11,787 genomes from 20 different serovars) and *S. aureus* (600 genomes) were run with mlst and stringMLST for ST-based classification. In the case of stringMLST, kmer lengths varied from 10 to 90 to identify the optimal value (highest percentage of agreement with the standard MLST approach), across all four species (y-axis). If both programs outputted identical ST calls (either number of missing/blank value), the call was defined as a match; otherwise, it was identified as a mismatch, and the percentage of agreement (x-axis, concordance) was calculated accordingly. The dashed line on the x-axis represents the percentage agreement for the kmer value of 35 which is used as a default parameter by stringMLST.

A.

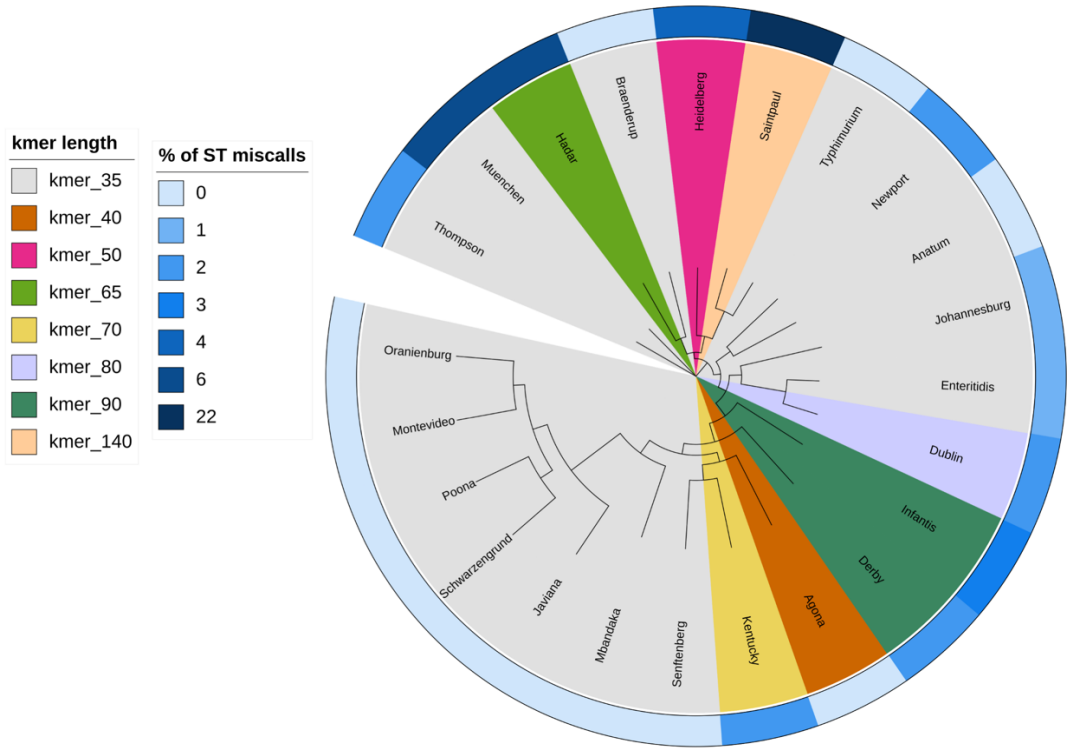
kmer length
kmer_35
kmer_40
kmer_50
kmer_65
kmer_70
kmer_80
kmer_90
kmer_140
% of ST miscalls
0
1
2
3
4
6
22
Heidelberg
Saintpaul
Typhimurium
Newport
Anatum
Johannesburg
Enteritidis
Dublin
Infantis
Derby
Agona
Kentucky
Senftenberg
Mbandaka
Javiana
Schwarzengrund
Poona
Montevideo
Oranienburg
Thompson
Muenchen
Hadar
Braenderup

B.

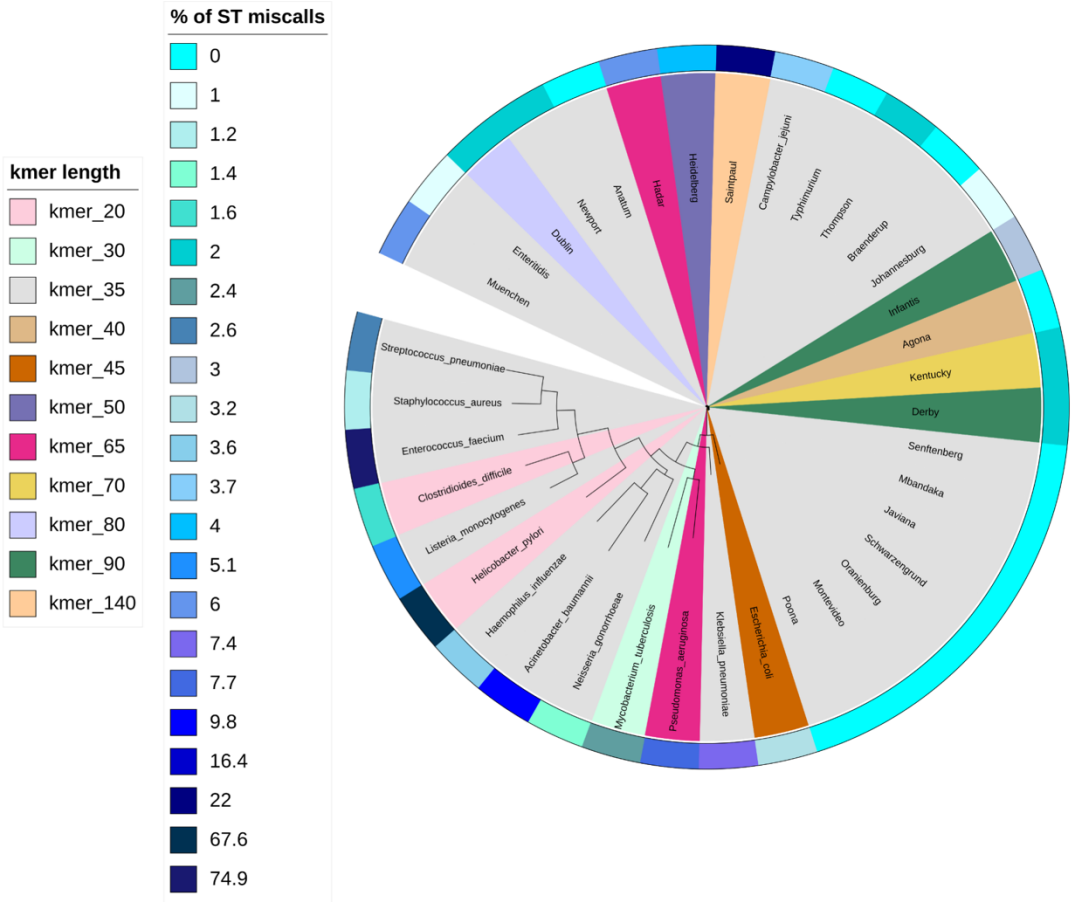
kmer length
kmer_20
kmer_30
kmer_35
kmer_40
kmer_45
kmer_50
kmer_65
kmer_70
kmer_80
kmer_90
kmer_140
% of ST miscalls
0
1
1.2
1.4
1.6
2
2.4
2.6
3
3.2
3.6
3.7
4
5.1
6
7.4
7.7
9.8
16.4
22
67.6
74.9
Saintpaul
Campylobacter_jejuni
Typhimurium
Thompson
Braenderup
Johannesburg
Infantis
Agona
Kentucky
Derby
Senftenberg
Mbandaka
Javiana
Schwarzengrund
Oranienburg
Montevideo
Poona
Escherichia_coli
Klebsiella_pneumoniae
Pseudomonas_aeruginosa
Mycobacterium_tuberculosis
Neisseria_gonorrhoeae
Acinetobacter_baumannii
Haemophilus_influenzae
Helicobacter_pylori
Listeria_monocytogenes
Clostridioides_difficile
Enterococcus_faecium
Staphylococcus_aureus
Streptococcus_pneumoniae
Muenchen
Enteritidis
Dublin
Newport
Anatum
Hadar
Heidelberg

Figure 7. Phylogeny-guided display of optimal kmer length and algorithmic performance when using stringMLST for ST mapping across bacterial species. (A) Phylogeny-based display of stringMLST results across the twenty-three zoonotic serovars of *Salmonella enterica* subsp. *enterica* lineage I (*S. enterica*). The branches are colored based on the optimal kmer length which gives the lowest percentage of ST miscalls (ST calls that returned missing/blank values for stringMLST). The outer ring present in the phylogeny is colored based on the corresponding ST miscall percentages associated with each optimal kmer length. The dataset used to identify the optimal kmer length and percentage of ST miscalls was composed of 2,300 genomes (100 genomes per serovar) and the phylogenetic tree was generated using twenty-three genomes (one of each serovar to facilitate data visualization); (B) Phylogeny-based display of stringMLST results across fourteen phylogenetic divergent bacterial pathogens, including twenty-three representative genomes across each zoonotic serovar of the *S. enterica* species. The tree branches are colored based on the optimal kmer length which minimizes the percentage of ST miscalls (ST calls that returned missing/blank values for stringMLST). The outer ring present in the phylogeny corresponds to ST miscall percentage associated with each optimal kmer length. The dataset used to identify the optimal kmer length and percentage of ST miscalls was composed of 14,000 genomes (1,000 genomes for each bacterial pathogen) and 2,300 *Salmonella* genomes (100 genomes per serovar). The phylogeny was ultimately generated using 37 genomes (one of each dataset used to facilitate visualization). All phylogeny-based visualization were generated using iTOL version 6.4.

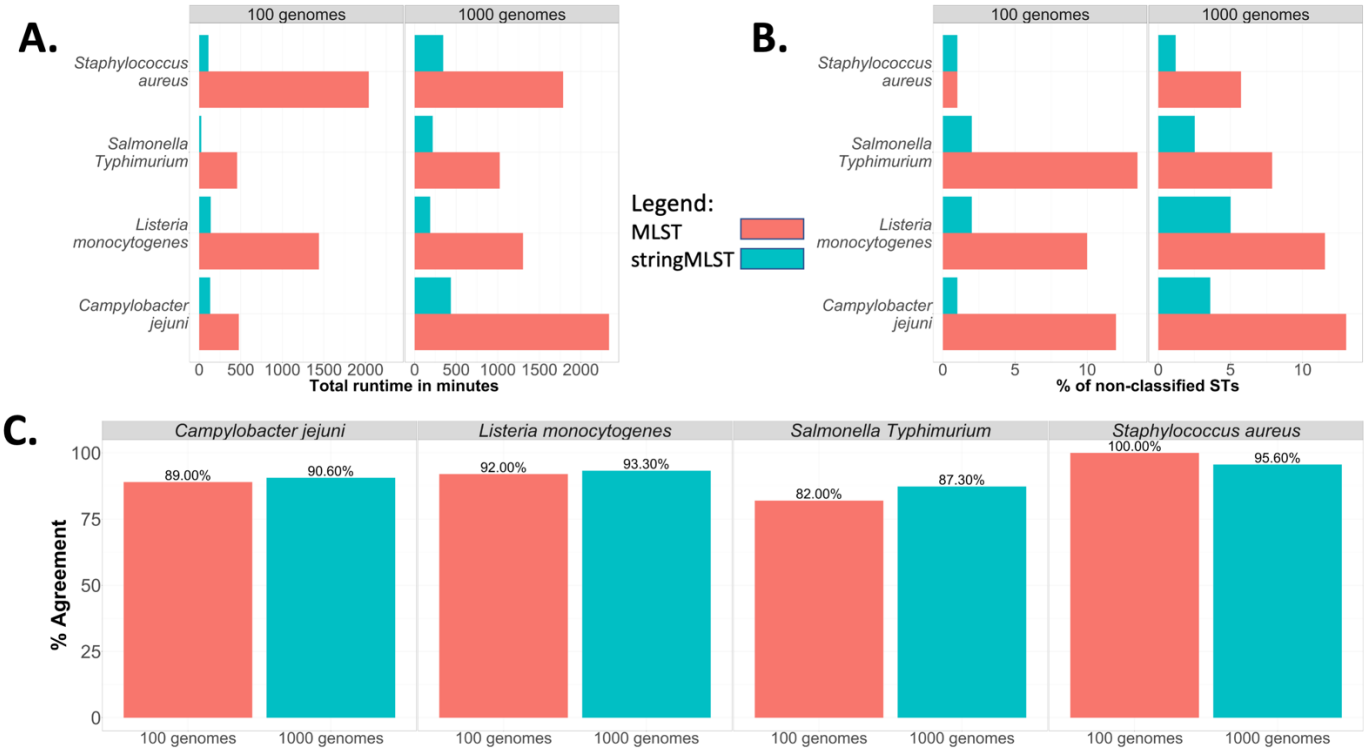

Figure 8. Comparison between the computational and statistical performance of mlst and stringMLST when using ProkEvo to run both programs.
Two subsets, one with 100 and the second one with 1,000 randomly chosen genomes, were selected from *C. jejuni*, *L. monocytogenes*, one major serovar of *S. enterica* (*S.* Typhimurium) and *S. aureus* to compare the performance of running mlst or stringMLST through ProkEvo. The performance and statistical metrics used for comparison were: (A) Total runtime of individual workflow in minutes; (B) Percentage of non-classified STs (ST calls that returned missing/blank values); and (C) Percentage of agreement (concordance) between programs ("good" or "bad" ST calls that matched between mlst and stringMLST).